Tanaka *et al.* Fig.4

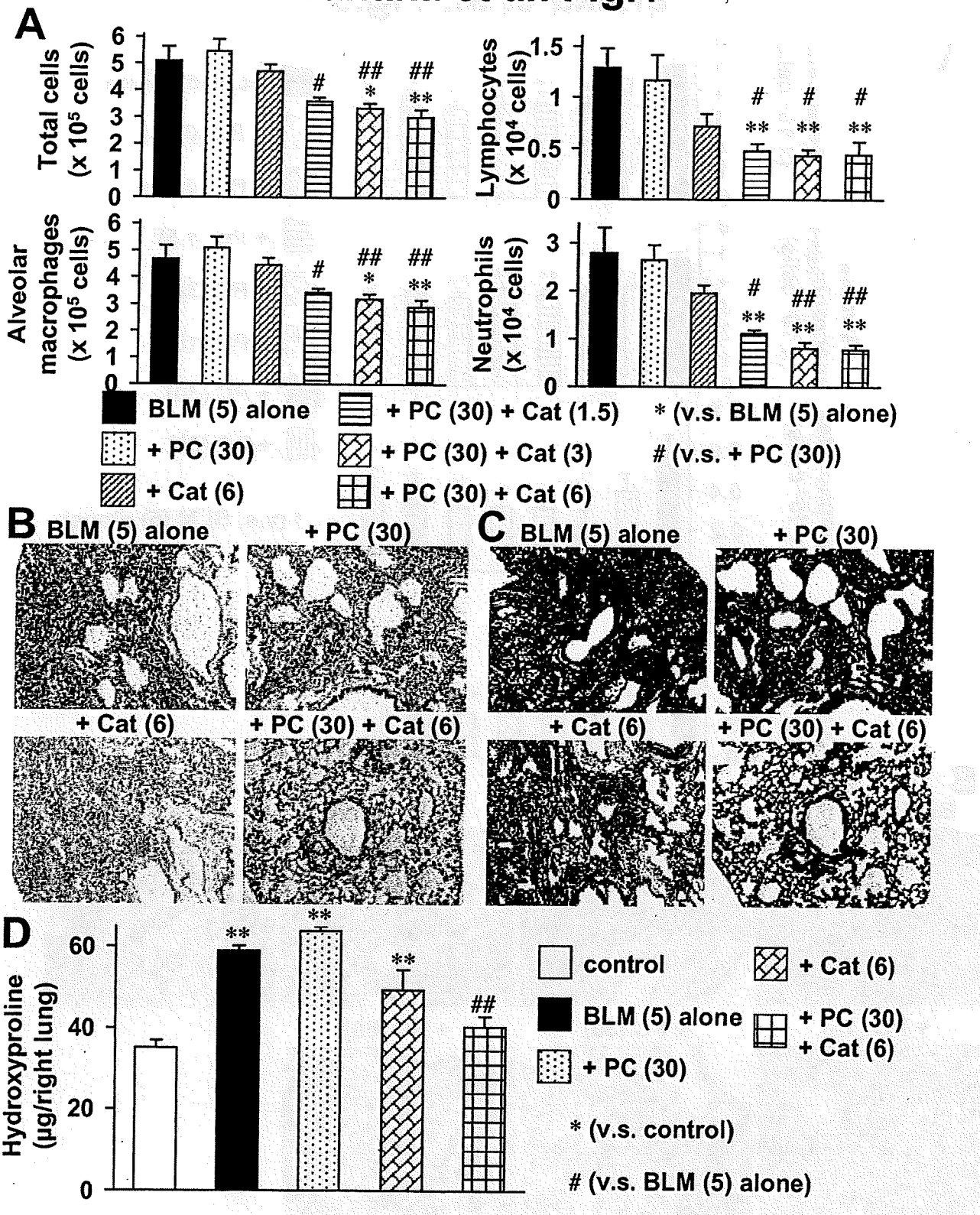

Tanaka *et al.* Fig.5

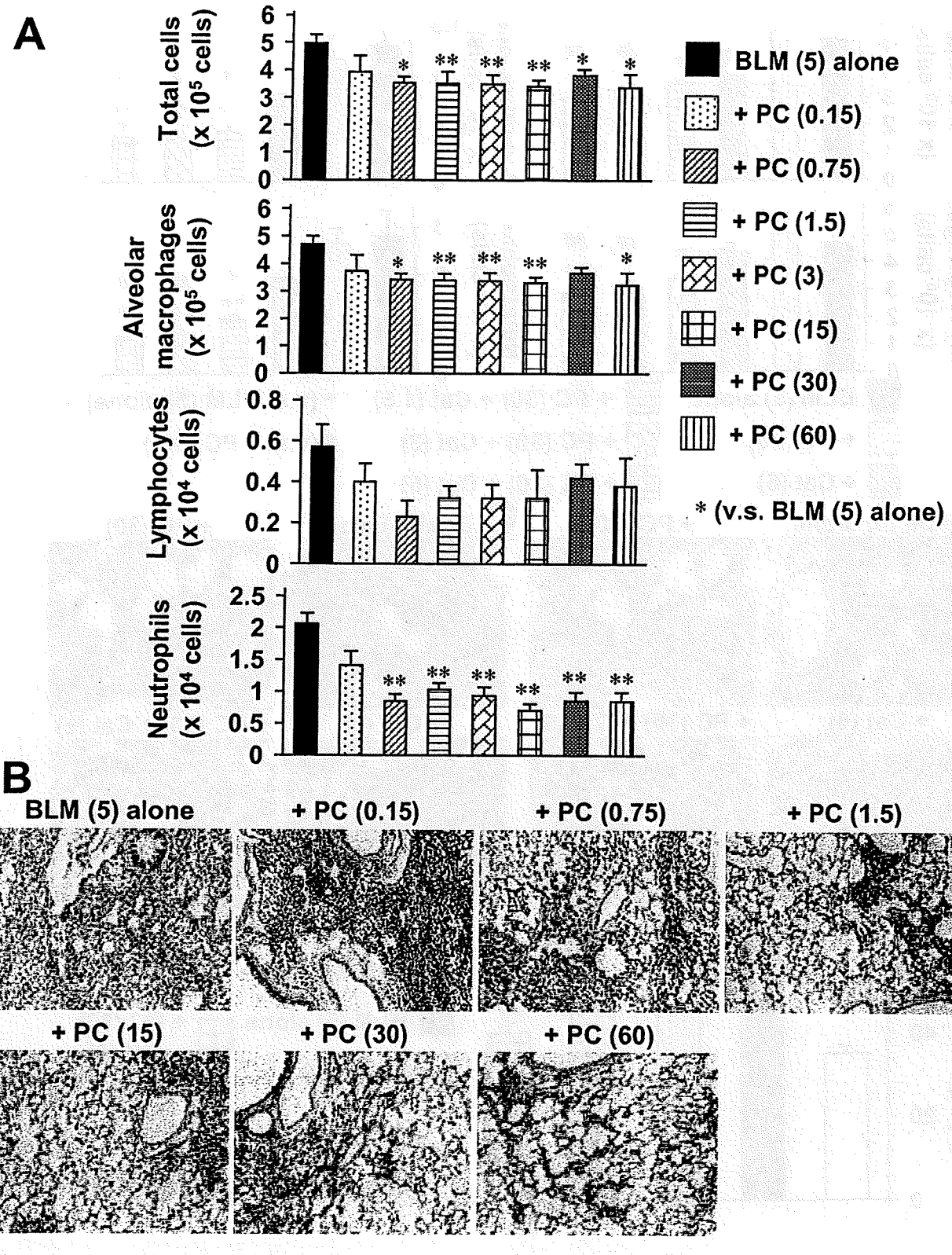

Tanaka *et al.* Fig.5

C

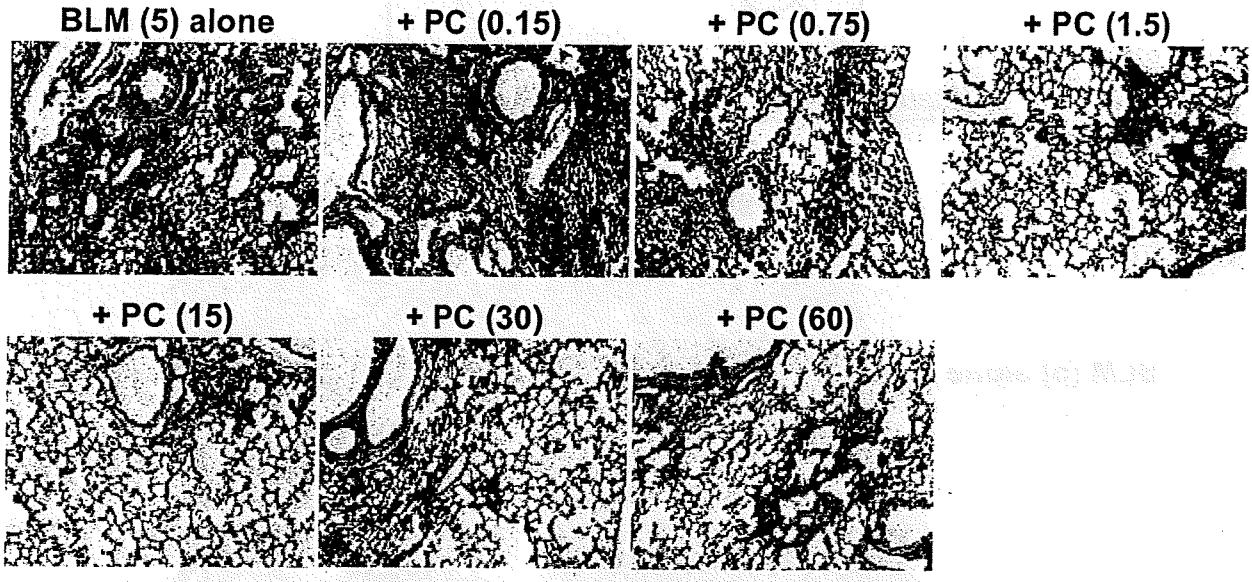

D

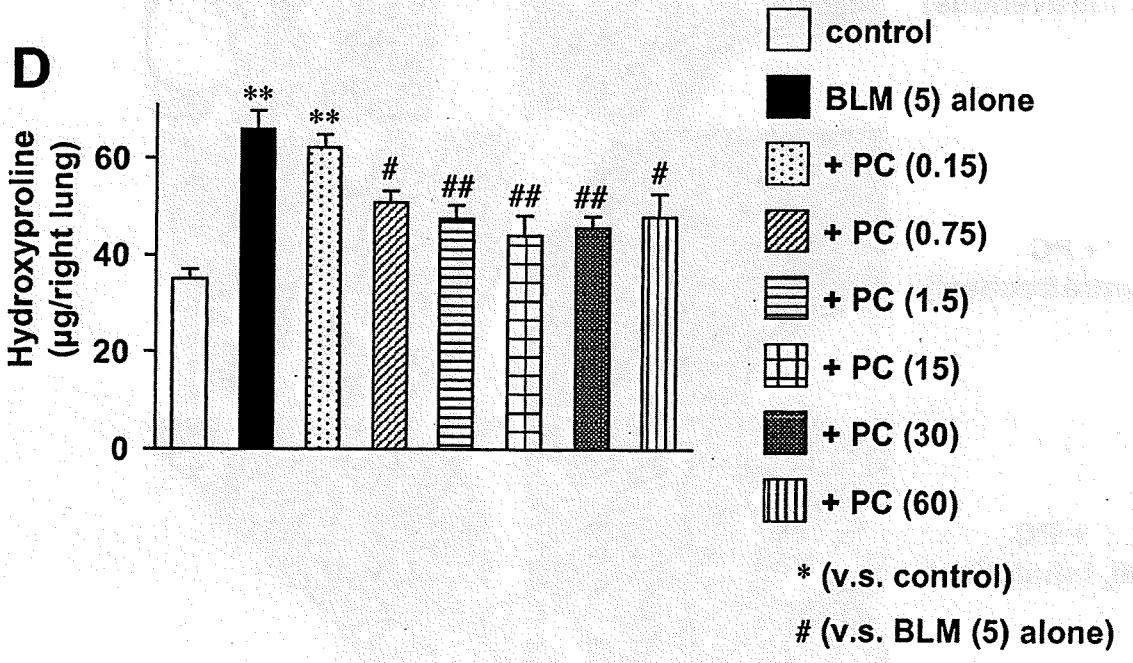

Tanaka *et al.* Fig.6

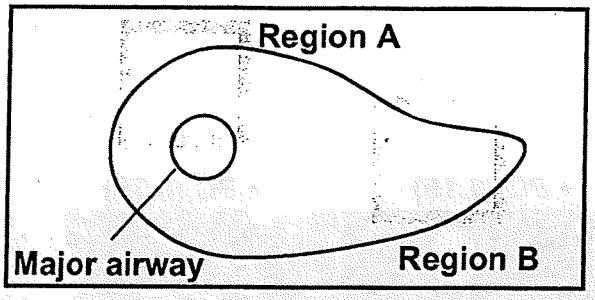

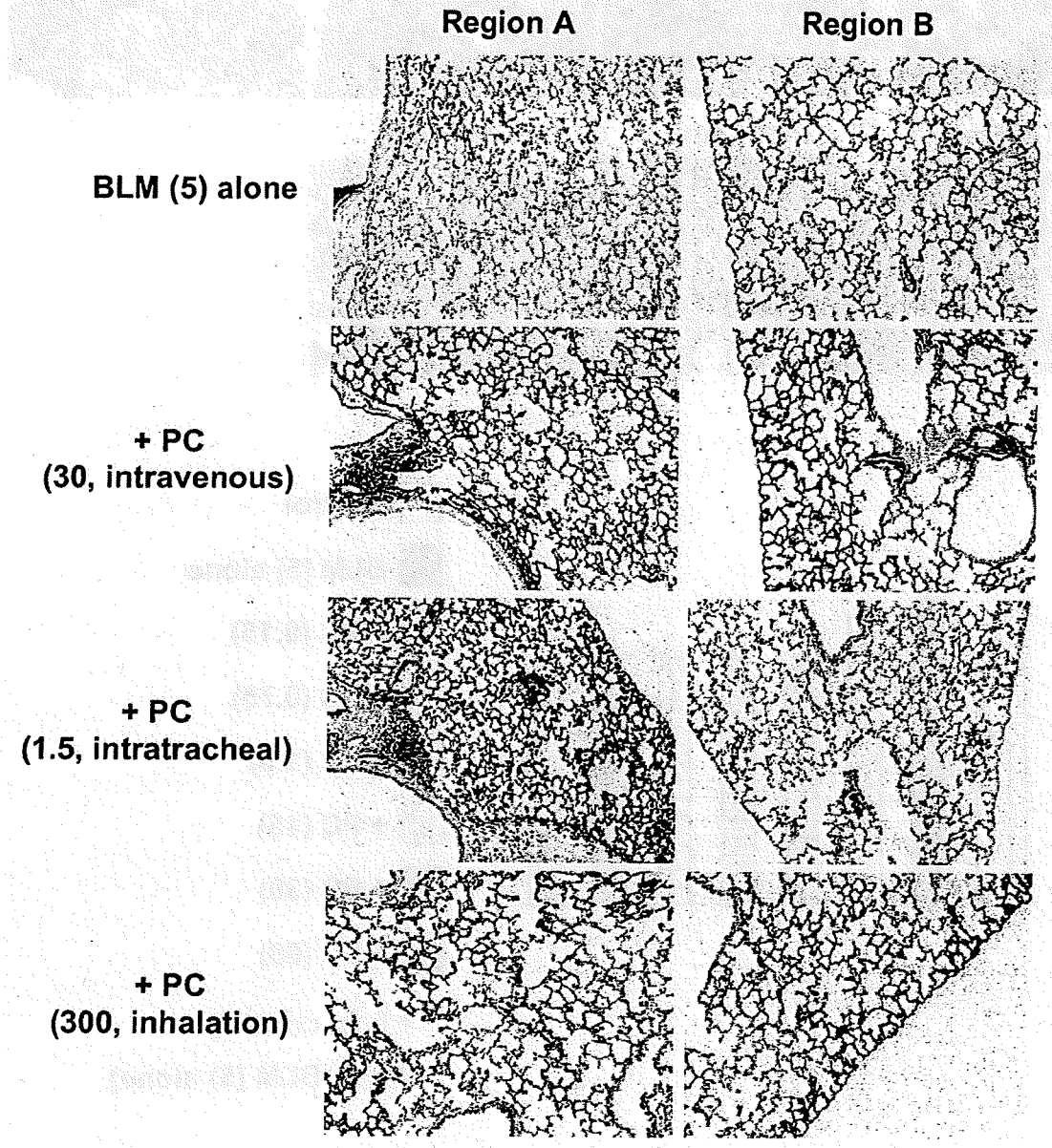

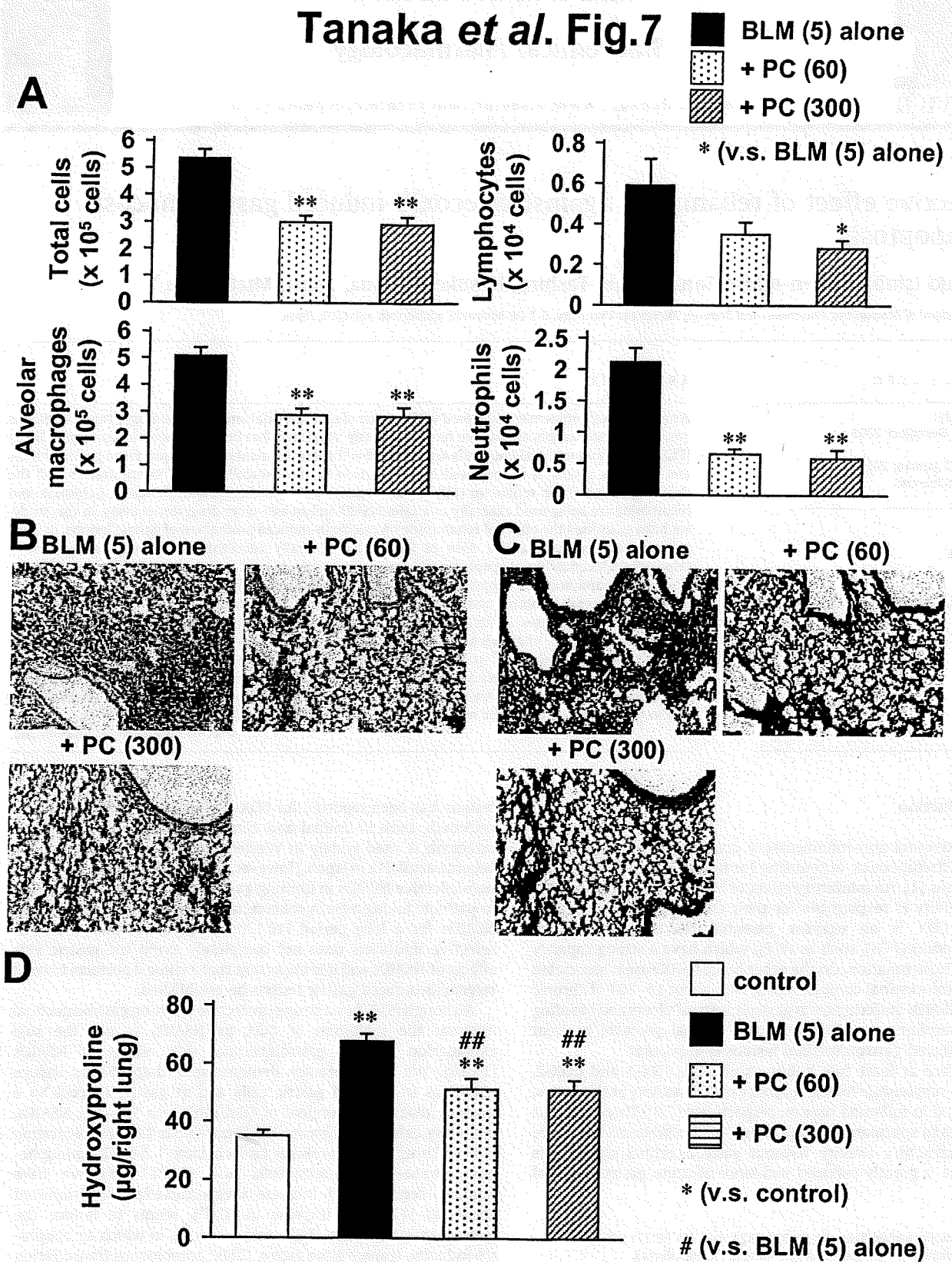
Tanaka et al. Fig.7
BLM (5) alone
+ PC (60)
+ PC (300)
A
Total cells (x 10⁵ cells)
Lymphocytes (x 10⁴ cells)
Alveolar macrophages (x 10⁵ cells)
Neutrophils (x 10⁴ cells)
* (v.s. BLM (5) alone)
B
BLM (5) alone
+ PC (60)
+ PC (300)
C
BLM (5) alone
+ PC (60)
+ PC (300)
D
Hydroxyproline (μg/right lung)
control
BLM (5) alone
+ PC (60)
+ PC (300)
* (v.s. control)
# (v.s. BLM (5) alone)

Biochemical Pharmacology xxx (2010) xxx–xxx

Contents lists available at ScienceDirect

Biochemical Pharmacology

journal homepage: www.elsevier.com/locate/biochempharm

Protective effect of rebamipide against celecoxib-induced gastric mucosal cell apoptosis

Tomoaki Ishihara, Ken-Ichiro Tanaka, Saki Tashiro, Kosuke Yoshida, Tohru Mizushima *

Graduate School of Medical and Pharmaceutical Sciences, Kumamoto University, 5-1 Oe-honmachi, Kumamoto 862-0973, Japan

ARTICLE INFO

Article history:
Received 3 December 2009

Accepted 25 January 2010
Available online xxx

Keywords:
Celecoxib
Rebamipide
Ulcer
Apoptosis
Voltage-dependent L-type Ca^{2+} channel

ABSTRACT

A major clinical problem encountered with the use of non-steroidal anti-inflammatory drugs (NSAIDs) is gastrointestinal complications. We have previously suggested that both decreases in prostaglandin E_2 (PGE_2) levels and mucosal apoptosis are involved in the development of NSAID-produced gastric lesions and that this apoptosis is mediated by an increase in the intracellular Ca^{2+} concentration and the resulting endoplasmic reticulum (ER) stress response and mitochondrial dysfunction. Celecoxib and rebamipide are being used clinically as a safer NSAID and an anti-ulcer drug, respectively. In this study, we have examined the effect of rebamipide on celecoxib-induced production of gastric lesions. In mice pre-administered with a low dose of indomethacin, orally administered rebamipide suppressed celecoxib-induced mucosal apoptosis and lesion production but did not decrease in PGE_2 levels in the stomach. Rebamipide also suppressed celecoxib-induced increases in intracellular Ca^{2+} concentration, the ER stress response, mitochondrial dysfunction and apoptosis *in vitro*. We also found that rebamipide suppresses the increases in intracellular Ca^{2+} concentration induced by an activator of voltage-dependent L-type Ca^{2+} channels and that another blocker of this channel suppresses celecoxib-induced increases in intracellular Ca^{2+} concentration. These results suggest that celecoxib activates voltage-dependent L-type Ca^{2+} channels and that rebamipide blocks this activation, resulting in suppression of celecoxib-induced apoptosis. We believe that this novel activity of rebamipide may play an important role in the protection of gastric mucosa against the formation of celecoxib-induced lesions.

1. Introduction

Non-steroidal anti-inflammatory drugs (NSAIDs) are a useful family of therapeutics, accounting for nearly 5% of all prescribed medications [1]. An inhibitory effect of NSAIDs on cyclooxygenase (COX) activity is responsible for their anti-inflammatory actions because COX is an enzyme essential for the synthesis of prostaglandins (PGs), such as PGE_2, which have a strong capacity to induce inflammation. On the other hand, NSAID use is associated with gastrointestinal complications, with about 15–30% of chronic users of NSAIDs suffering from gastrointestinal ulcers and bleeding [2–6]. Therefore, establishment of a clinical protocol to treat NSAID-induced gastrointestinal lesions is important.

There are at least two subtypes of COX, COX-1 and COX-2, which are responsible for the majority of COX activity at the gastric mucosa and in inflamed tissues, respectively [7,8]. Therefore, it is reasonable to speculate that selective COX-2 inhibitors could have anti-inflammatory activity without gastrointestinal side effects [7]. In fact, a greatly reduced incidence of acute gastroduodenal lesions has been reported for COX-2-selective inhibitors, such as celecoxib, both in animal and clinical studies [9–12] and thus, celecoxib is used widely in Western countries and recently has become available in Japan. However, the superiority of celecoxib to non-selective NSAIDs in limiting gastric side effects is not as clear in patients taking aspirin concomitantly or in patients using such NSAIDs for a long period [10,13,14]. Therefore, use of COX-2-selective inhibitors does not completely avoid the gastric side effects of NSAIDs and it is important that a clinical protocol to treat celecoxib-induced gastric lesions be established.

Although PGE_2 has a strong protective effect on gastrointestinal mucosa, the inhibition of COX by NSAIDs is not the sole explanation for the gastrointestinal side effects of NSAIDs [15,16]. We have recently demonstrated that NSAIDs induce apoptosis in cultured gastric cells and at gastric mucosa in a manner that is independent of COX inhibition [17–21]. NSAIDs, including celecoxib, increase the intracellular Ca^{2+} concentration $[Ca^{2+}]_i$. Using the intracellular Ca^{2+} chelator 1,2-bis(2-aminophenoxy)ethane-N,N,N′N′-tetraacetic acid (BAPTA-AM), we have found evidence that this increase is responsible for NSAID-induced apoptosis [17]. This increase in $[Ca^{2+}]_i$ seems to induce the endoplasmic reticulum (ER) stress response, in which an apoptosis-inducing transcription factor, C/EBP homologous transcription

* *Corresponding author.* Tel.: +81 96 371 4323; fax: +81 96 371 4323.
E-mail address: mizu@gpo.kumamoto-u.ac.jp (T. Mizushima).

0006-2952/$ – see front matter © 2010 Published by Elsevier Inc.
doi:10.1016/j.bcp.2010.01.030

Please cite this article in press as: Ishihara T, et al. Protective effect of rebamipide against celecoxib-induced gastric mucosal cell apoptosis. Biochem Pharmacol (2010), doi:10.1016/j.bcp.2010.01.030

factor (*chop*), is induced and we have previously shown, *chop* is essential for NSAID-induced apoptosis [18]. With the aid of activating transcription factor 4 (*atf4*), *chop* induces expression of p53 up-regulated modulator of apoptosis (*puma*) and the resulting activation of Bax [22]. We have already shown that both *puma* and Bax play important roles in NSAID-induced mitochondrial dysfunction, activation of caspases and apoptosis [17,22–24]. Furthermore, we have suggested that both COX inhibition (resulting in a decrease in gastric PGE_2 levels) and gastric mucosal apoptosis are required for the formation of NSAID-induced gastric lesions *in vivo* [21,25,26]. Therefore, it will be important to consider protection of gastric mucosal cells against celecoxib-induced apoptosis when establishing a clinical protocol to treat celecoxib-induced gastric lesions.

Rebamipide is an anti-ulcer drug used in Asian countries [27,28]. Both animal and clinical studies have revealed that rebamipide prevents the formation of NSAID-induced gastric lesions [27–30]; however, no clinical or animal data regarding the effect of rebamipide on celecoxib-induced gastric lesions have been reported. Rebamipide has various gastroprotective mechanisms, such as decreasing reactive oxygen species (ROS) and up-regulating COX-2 expression; this latter function increases gastric PGE_2 levels, which in turn stimulates mucus secretion and gastric mucosal blood flow [27,31–33]. Furthermore, the protective effect of rebamipide on cells against indomethacin-induced apoptosis has been reported *in vitro* [34,35]. However, the effect of rebamipide on celecoxib-induced apoptosis has not been reported. In this study, we have obtained *in vivo* data suggesting that orally administered rebamipide suppresses the formation of celecoxib-produced gastric lesions through suppression of mucosal apoptosis. It was also found that rebamipide suppresses the celecoxib-induced increase in $[Ca^{2+}]_i$, the ER stress response, mitochondrial dysfunction and apoptosis *in vitro*. We suggest that rebamipide achieves these effects through inhibition of a voltage-dependent L-type Ca^{2+} channel.

2. Materials and methods

2.1. Chemicals and animals

RPMI 1640 was obtained from Nissui Pharmaceutical Co (Osaka, Japan). Rebamipide was kindly provided by Otsuka Pharmaceutical Co (Tokushima, Japan). Pluronic F127, fluo-3/AM, 4′, 6-diamidino-2-phenylindole dihydrochloride (DAPI) and BAPTA-AM were obtained from Dojindo Co (Kumamoto, Japan). Paraformaldehyde, fetal bovine serum (FBS), tunicamycin, thapsigargin, ionomycin, Hoechst 33258 and (S)-(-)-BAY K 8644 (BAYK 8644) were obtained from Sigma (St. Louis, MO). Indomethacin, ibuprofen, diclofenac and nifedipine were obtained from Wako Co (Osaka, Japan). Celecoxib was from LKT Laboratories Inc (St Paul, MN). A PGE_2 enzyme immuno assay (EIA) kit was purchased from Cayman Chemical (Ann Arbor, MI). Antibodies against *puma* or the N-terminal region of Bax (Bax N20) and actin were purchased from ProSci Inc (Poway, CA) or Santa Cruz Biotechnology (Santa Cruz, CA), respectively. An antibody against cytochrome c was from PharMingen (San Jose, CA). Terminal deoxynucleotidyl transferase (TdT) was obtained from TOYOBO (Osaka, Japan). Mayer's hematoxylin, 1% eosin alcohol solution and mounting medium for histological examination (Malinol) were from MUTO Pure Chemicals (Tokyo, Japan). Biotin 14-ATP, Alexa Fluor 488 goat anti-rabbit immunoglobulin G and Alexa Fluor 488 conjugated with streptavidin were purchased from Invitrogen (Carlsbad, CA). Mounting medium (VECTASHIELD) was from Vector Laboratories (Burlingame, CA). The RNeasy kit was obtained from QIAGEN (Valencia, CA), the first-strand cDNA synthesis kit was from Takara (Kyoto, Japan), and iQ SYBR Green Supermix was from Bio-Rad (Hercules, CA). Wild-type mice (C57/BL6) (8–10 weeks of age and 25 to 30 g) were used. The experiments and procedures described here were carried out in accordance with the Guide for the Care and Use of Laboratory Animals as adopted and promulgated by the National Institutes of Health (Bethesda, MD) and were approved by the Animal Care Committee of Kumamoto University.

2.2. Gastric damage assay

The gastric ulcerogenic response was examined as described previously [25], with some modifications. Mice fasted for 18 h were intravenously administered indomethacin in PBS via the tail vein and 1 h later, orally administered celecoxib in 1% methylcellulose in a volume of 10 ml/kg. In some experiments, mice were orally administered rebamipide in 0.5% carboxymethylcellulose in a volume of 10 ml/kg 1 h before the administration of indomethacin. Eight hours after the administration of celecoxib, the animals were sacrificed, after which their stomachs were removed and the areas of the gastric mucosal lesions were measured by an observer unaware of the treatment they had received. Calculation of the scores involved measuring the area of all the lesions in square millimetres and summing the values to give an overall gastric lesion index. The gastric PGE_2 level was determined by EIA according to the manufacturer's instructions.

2.3. Cell culture and assay for apoptosis and K^+ efflux

Human gastric adenocarcinoma (AGS) cells were cultured in RPMI 1640 medium supplemented with 10% FBS, 100 U/ml penicillin and 100 μg/ml streptomycin in a humidified atmosphere of 95% air with 5% CO_2 at 37 °C. Cells were exposed to celecoxib by changing the medium. Cells were cultured for 24 h and then used in experiments. Apoptosis was monitored by fluorescence-activated cell sorting (FACS) analysis, chromatin condensation by staining with Hoechst dye 33258 and caspase-3-like activity as previously described [18,20,23]. K^+ efflux from cells was monitored as previously described [17,36].

2.4. Real-time RT-PCR analysis

Total RNA was extracted from AGS cells using an RNeasy kit according to the manufacturer's protocol. Samples (2.5 μg of RNA) were reverse-transcribed using a first-strand cDNA synthesis kit according to the manufacturer's instructions. Synthesized cDNA was used in real-time RT-PCR (Bio-Rad Chromo 4 system) experiments using iQ SYBR Green Supermix and analysed with Opticon Monitor software according to the manufacturer's instructions. The real-time PCR cycle conditions were 95 °C for 3 min, followed by 44 cycles at 95 °C for 10 s and at 60 °C for 60 s. Specificity was confirmed by electrophoretic analysis of the reaction products and by inclusion of template- or reverse transcriptase-free controls. To normalize the amount of total RNA present in each reaction, actin cDNA was used as an internal standard.

Primers were designed using the Primer3 website (http://frodo.wi.mit.edu/cgi-bin/primer3/primer3_www.cgi). The primers used were (name, forward primer and reverse primer): *atf4*, 5′-tcaaacctcatgggttctcc-3′ and 5′-gtgtcatccaacgtggtcag-3′; *chop*, 5′-tgcctttctcttcggacact-3′ and 5′-tgtgacctctgctggttctg-3′; *puma*, 5′-gacgacctcaacgcacagta-3′ and 5′-ggagtcccatgatgagattgt-3′; *actin*, 5′-tgcctttctcttcggacact-3′ and 5′-tgtgacctctgctggttctg-3′.

2.5. Immunoblotting analysis

Total protein was extracted as described previously [37]. The protein concentration of each sample was determined by the

Please cite this article in press as: Ishihara T, et al. Protective effect of rebamipide against celecoxib-induced gastric mucosal cell apoptosis. Biochem Pharmacol (2010), doi:10.1016/j.bcp.2010.01.030

Bradford method [38]. Samples were applied to polyacrylamide SDS gels and subjected to electrophoresis, after which the proteins were immunoblotted with appropriate antibodies.

2.6. Histological and TdT-mediated biotinylated UTP Nick End Labelling (TUNEL) analyses

Gastric tissue samples were fixed in 4% buffered paraformaldehyde and embedded in paraffin before being cut into 4 μm sections.

For histological examination (hematoxylin and eosin [H & E] staining), sections were stained first with Mayer's hematoxylin and then with 1% eosin alcohol solution. Samples were mounted with Malinol and inspected with the aid of an Olympus BX51 microscope.

For TUNEL assay, sections were incubated first with proteinase K for 15 min at 37 °C, then with TdT and biotin 14-ATP for 1 h at 37 °C, and finally with Alexa Fluor 488 conjugated with streptavidin for 1 h. Samples were mounted with VECTASHIELD and inspected using fluorescence microscopy (Olympus BX51).

2.7. Immunostaining of cells

Cells were cultured on 4-well Lab-Tek II glass slides (Nunc). After fixation with 4% buffered paraformaldehyde for 20 min and permeabilization with 0.5% Triton X-100 for 5 min, non-specific binding sites were blocked with 3% BSA for 30 min. Immunostaining to detect the active form of Bax was performed with a polyclonal antibody (Bax N20) and Alexa Fluor 488 goat anti-rabbit immunoglobulin G. Cells were simultaneously stained with DAPI (5 μg/ml). Cells were mounted with VECTASHIELD and inspected using fluorescence microscopy (Olympus BX51).

2.8. Measurement of intracellular Ca^{2+} Levels

Intracellular Ca^{2+} levels were monitored as previously described [17]. Cells were incubated with 4 μM fluo-3/AM in the assay buffer (115 mM NaCl, 5.4 mM KCl, 1.8 mM $CaCl_2$, 0.8 mM $MgCl_2$, 20 mM HEPES, 13.8 mM glucose, 0.1% BSA, 0.04% Pluronic F127 and 2 mM probenecid) for 40 min at 37 °C. For Ca^{2+}-free conditions, a modified assay buffer (115 mM NaCl, 5.4 mM KCl, 5 mM EGTA, 20 mM HEPES, 13.8 mM glucose and 2 mM probenecid) was used. After washing, cells were suspended in the assay buffer without BSA and Pluronic F127. Fluo-3 fluorescence of cells was measured with a HITACHI F-4500 spectrofluorophotometer. Maximum and minimum fluorescence values (F_{max} and F_{min}) were obtained by adding 10 μM ionomycin and 10 μM ionomycin plus 5 mM EGTA (in Ca^{2+}-free medium), respectively. The intracellular Ca^{2+} level was calculated according to the equation $[Ca^{2+}]_i = K_d(F - F_{min})/(F_{max} - F)$, where K_d

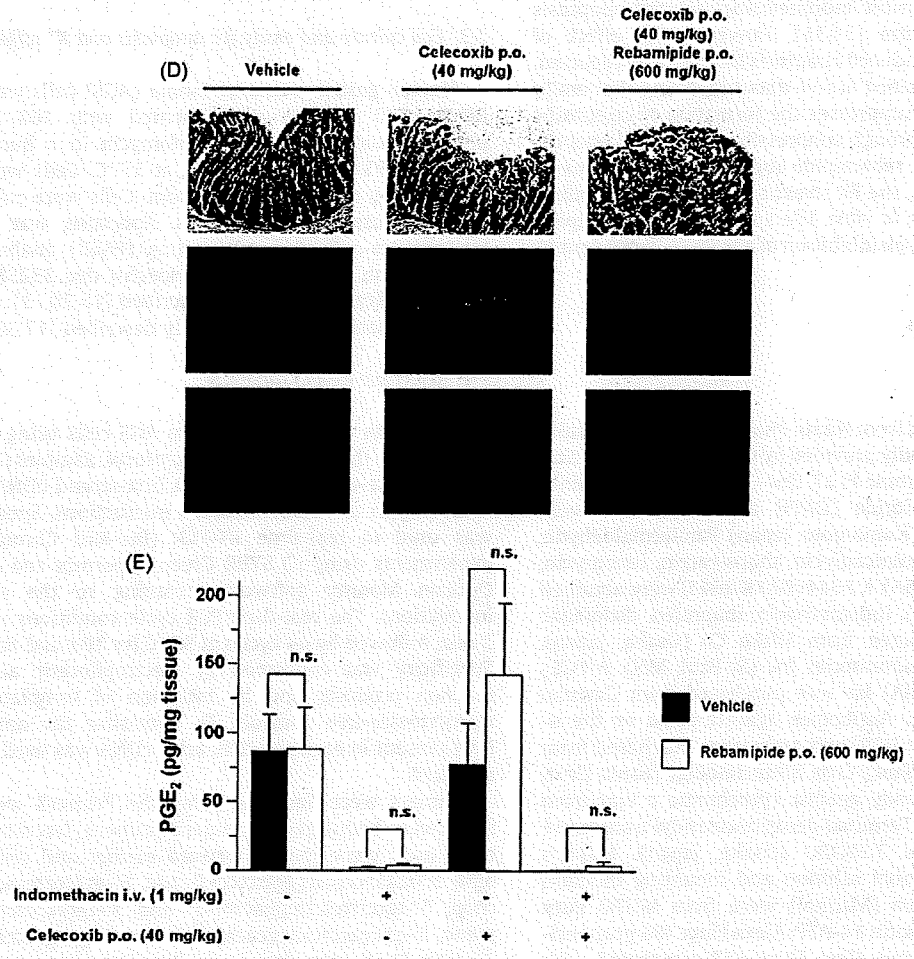

Fig. 1. Effect of rebamipide on celecoxib-induced gastric lesions and apoptosis *in vivo*.
Mice were intravenously (IV) administered 1 mg/kg indomethacin or vehicle and, after 1 h, mice were orally (p.o.) administered 40 mg/kg celecoxib or vehicle (A–E). Mice were orally administered the indicated dose (B) or 600 mg/kg (C–E) of rebamipide or vehicle 1 h before the administration of indomethacin (B, C, E) or celecoxib (D). After 8 h from the administration of celecoxib, the stomach was removed and scored for hemorrhagic damage as described in the experimental procedures (A, B). After 8 h, sections of gastric tissues were prepared and subjected to H & E staining (upper panels), TUNEL assay (middle panels) and DAPI staining (lower panels) (C, D). After 4 h, the gastric PGE_2 level was determined by EIA (E). Values are mean ± S.E.M. ($n = 3$–8). $^{**}P < 0.01$; $^{*}P < 0.05$; n.s., not significant (A, B, E). Scale bar, 100 μm.

Please cite this article in press as: Ishihara T, et al. Protective effect of rebamipide against celecoxib-induced gastric mucosal cell apoptosis. Biochem Pharmacol (2010), doi:10.1016/j.bcp.2010.01.030

is the apparent dissociation constant (400 nM) of the fluorescent dye-Ca^{2+} complex.

2.9. Statistical analysis

The Tukey test or the Student's *t*-test for unpaired results was used to evaluate differences between more than three groups or between two groups, respectively. Differences were considered to be significant for values of $P < 0.05$.

3. Results

3.1. Effect of rebamipide on the celecoxib-induced gastric ulcerogenic response

It is known that oral administration of celecoxib alone produces few gastric lesions in animals [39]. Based on our idea that both COX inhibition (resulting in a decrease in gastric PGE_2 levels) and gastric mucosal apoptosis are required for the formation of NSAID-induced gastric lesions *in vivo*, we recently showed that gastric lesions develop in a manner that is dependent on oral administration of cytotoxic COX-2-selective inhibitors, such as celecoxib (for induction of gastric mucosal apoptosis), in mice pre-administered intravenously with low doses of indomethacin (for decrease in gastric PGE_2 levels) [25]. In this study we have confirmed these results (Fig. 1A) and have found that oral pre-administration of rebamipide (300 or 600 mg/kg) suppresses this gastric lesion production (1 mg/kg indomethacin and 40 mg/kg celecoxib) in a dose-dependent manner (Fig. 1B). Histological analysis has revealed that gastric mucosal damage (crypt loss and infiltration of leukocytes) was observed in sections from indomethacin/celecoxib-administered mice and that this damage was suppressed by the pre-administration of rebamipide (600 mg/kg) (Fig. 1C).

As mentioned above, both decreases in PGE_2 levels and mucosal apoptosis play important roles in the development of NSAID-produced gastric lesions [25]. The level of gastric mucosal apoptosis was determined by TUNEL assay. An increase in TUNEL-positive (apoptotic) cells was observed at the gastric mucosa of indomethacin/celecoxib-administered mice and pre-administration of rebamipide (600 mg/kg) clearly suppressed this increase (Fig. 1C). Weak but significant apoptosis was observed at the gastric mucosa of mice treated with celecoxib alone (Fig. 1D) but not in those treated with indomethacin alone (data not shown), and this apoptosis was suppressed by pre-administration of rebamipide (Fig. 1D). These results suggest that administration of celecoxib rather than indomethacin is responsible for the apoptosis shown in Fig. 1C and that rebamipide somehow suppresses this celecoxib-induced apoptosis. On the other hand, pre-administration with rebamipide (600 mg/kg) did not affect gastric PGE_2 levels under any conditions (Fig. 1E). The level was decreased by intravenous administration of indomethacin but not by oral administration of celecoxib, as described previously [25]. These results suggest that rebamipide protects gastric mucosa against the formation of indomethacin/celecoxib-produced gastric lesions by inhibiting celecoxib-induced apoptosis rather than by inhibiting indomethacin-induced decreases in gastric PGE_2 levels.

3.2. Mechanism for protection by rebamipide against celecoxib-induced apoptosis in vitro

To understand the molecular mechanism governing rebamipide-conferred protection against celecoxib-induced apoptosis, we first tried to reproduce this phenomenon in cultured AGS cells. FACS analysis revealed that pre-treatment of cells with rebamipide (25–1000 μM) suppressed celecoxib-induced apoptosis in a dose-dependent manner (Fig. 2A). The anti-apoptotic effect of rebamipide (250 μM) was also confirmed by chromatin condensation assay and measurement of caspase-3-like activity (Fig. 2B and C). The results, shown in Fig. 2, suggest that rebamipide directly protects gastric cells against celecoxib-induced apoptosis. We also found that rebamipide did not affect apoptosis induced by NSAIDs other than celecoxib (diclofenac or ibuprofen) (data not shown). This result may be related to the observation that rebamipide did not affect the increase in $[Ca^{2+}]_i$ induced by diclofenac or ibuprofen (see Fig. 5B).

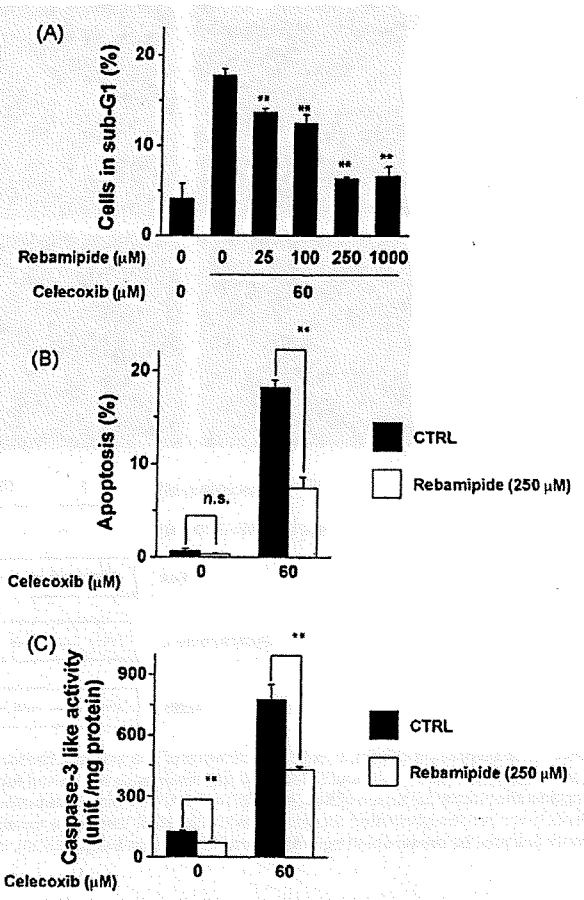

Fig. 2. Effect of rebamipide on celecoxib-induced apoptosis.
AGS cells were incubated with or without (CTRL) the indicated concentration of rebamipide for 1 h and further incubated with or without 60 μM celecoxib for 24 h (A–C). Apoptotic cell number (cells in sub-G1 phase) was determined by FACS (A). Cells were stained with Hoechst dye 33258 and cells with condensed chromatins were counted (1200–1600 total cells) (B). Caspase-3-like activity was measured (C). Values are mean ± S.D. ($n = 3$). $^{**}P < 0.01$; n.s., not significant (A–C).

As described above, celecoxib-induced apoptosis is mediated by the sequential induction of various cellular phenomena (increase in $[Ca^{2+}]_i$, ER stress response, activation of Bax, mitochondrial dysfunction and activation of caspases). Next, we examined which step of this apoptotic pathway is affected by rebamipide.

We have previously reported that activation of Bax, through its conformational change and resulting translocation from the cytosol to mitochondria, is responsible for celecoxib-induced mitochondrial dysfunction and apoptosis [22]. The effect of rebamipide on activation of Bax was tested by immunostaining analysis using an antibody that specifically recognizes only the active form of Bax. This antibody can recognize only the active form in the immunostaining assay but recognize all forms of Bax in the immunoblotting assay due to the denaturation of proteins in the latter assay [40]. As shown in Fig. 3A and B, the active form of Bax was observed in celecoxib (60 μM)-treated cells and the level

Please cite this article in press as: Ishihara T, et al. Protective effect of rebamipide against celecoxib-induced gastric mucosal cell apoptosis. Biochem Pharmacol (2010), doi:10.1016/j.bcp.2010.01.030

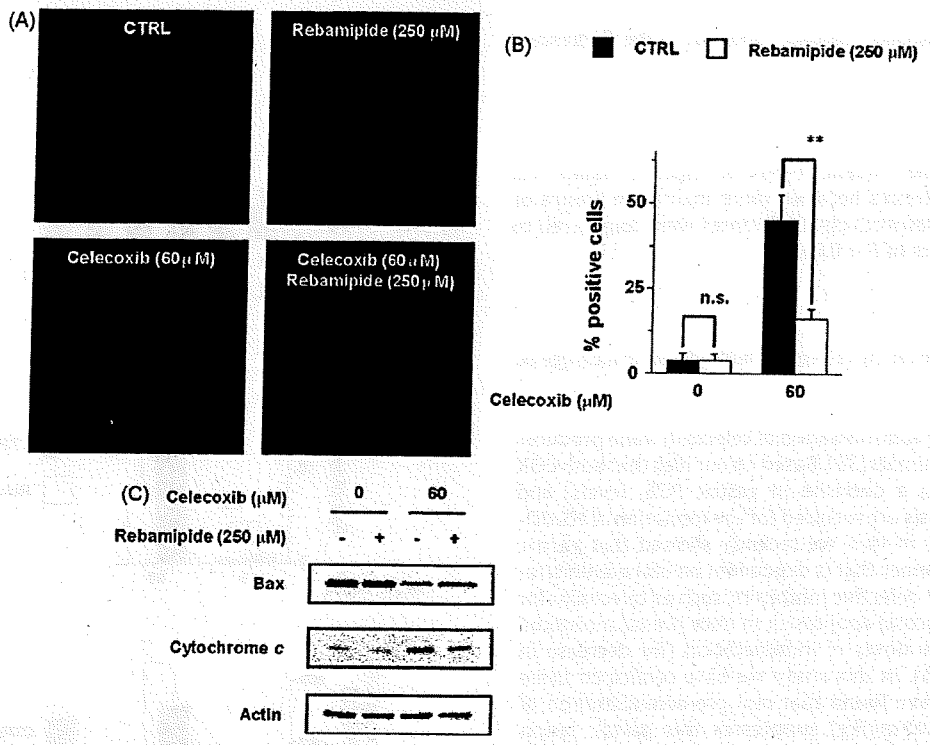

Fig. 3. Effect of rebamipide on celecoxib-induced activation of Bax and mitochondrial dysfunction.
AGS cells were incubated with or without (CTRL) 250 μM rebamipide for 1 h and further incubated with or without 60 μM celecoxib for 18 h (A–C). Immunostaining with antibody against the N-terminal region of Bax (Bax N20) and DAPI staining were performed as described in the experimental procedures. Scale bar, 50 μm (A). Approximately 400–600 cells were randomly counted for staining with Bax N20. Values are mean ± S.D. ($n = 3$). $^{**}P < 0.01$; n.s., not significant (B). After subcellular fractionation, cytosol fractions were analysed by immunoblotting with an antibody against Bax (Bax N20), cytochrome *c* or actin.

of the active form of Bax decreased in cells pre-treated with rebamipide (250 μM), suggesting that rebamipide suppresses celecoxib-dependent activation (conformational change) of Bax. As shown in Fig. 3C, the amount of Bax or cytochrome *c* in the cytosol fractions decreased or increased, respectively, in the presence of celecoxib (60 μM) and these alterations were suppressed by pre-treatment of the cells with rebamipide (250 μM), suggesting that rebamipide suppresses celecoxib-induced translocation of Bax and the resulting mitochondrial dysfunction.

We previously reported that in the pathway for celecoxib-induced apoptosis, the ER stress response, and particularly the up-regulation of *puma* expression, induces activation of Bax [22]. As shown in Fig. 4A and B, treatment of cells with celecoxib (60 μM) up-regulated the expression of *puma* at both mRNA and protein levels and this up-regulation was partially suppressed by pre-treatment of the cells with rebamipide (250 μM). We previously reported that up-regulation of expression of *atf4* and *chop*, both of which are transcription factors related to the ER stress response, is responsible for celecoxib-induced expression of *puma*. Here we have shown that celecoxib (60 μM) up-regulates the expression of *atf4* and *chop* mRNAs and that this up-regulation is partially suppressed by pre-treatment of cells with rebamipide (250 μM) (Fig. 4A). The results presented in Fig. 4 suggest that rebamipide suppresses the celecoxib-induced ER stress response.

We previously reported that NSAIDs increase $[Ca^{2+}]_i$ and suggested that this increase induces the ER stress response by showing that BAPTA-AM suppresses the response [17,22–24]. Here we have examined the effect of rebamipide (250 μM) on celecoxib (60 μM)-induced increases in $[Ca^{2+}]_i$ with Ca^{2+}-containing medium and found that rebamipide clearly suppresses this increase (Fig. 5A). On other hand, rebamipide did not affect increases in $[Ca^{2+}]_i$ induced by diclofenac (0.8 mM) or ibuprofen (2 mM) (Fig. 5B). Since indomethacin absorbs fluo-3 fluorescence (530 nm) [17], we could not measure the intracellular Ca^{2+} level in the presence of indomethacin by this assay system. We have confirmed that as well as rebamipide, BAPTA-AM (50 nM) suppresses celecoxib-dependent up-regulation of expression of ER stress response-related genes and have found that in the presence of BAPTA-AM, rebamipide does not further suppress celecoxib-dependent up-regulation of expression of these genes (Fig. 5C). This suggests that rebamipide shares a mechanism for suppressing the ER stress response with BAPTA-AM; in other words, that rebamipide suppresses the ER stress response through decreasing $[Ca^{2+}]_i$.

We then examined the effect of rebamipide on the increases in $[Ca^{2+}]_i$ induced by chemicals other than celecoxib, such as thapsigargin (an inhibitor of the sarcoplasmic/ER Ca^{2+} ATPase [SERCA]) and ionomycin (a Ca^{2+} ionophore). As shown in Fig. 6A, rebamipide did not affect the increase in $[Ca^{2+}]_i$ induced by thapsigargin (1 nM) or ionomycin (2 μM). We also found that rebamipide did not suppress (but in some cases actually stimulated) the up-regulation of expression of ER stress response-related genes induced by not only these two chemicals but also by tunicamycin (0.1 μg/ml), an inhibitor of N-glycosylation that does not affect $[Ca^{2+}]_i$ (Fig. 6B). These results suggest that the inhibitory effect of rebamipide on the ER stress response and increase in $[Ca^{2+}]_i$ is not observed generally but is specific for those induced by celecoxib.

3.3. Mechanism for the inhibitory effect of rebamipide on celecoxib-induced Increases in $[Ca^{2+}]_i$

Various mechanisms have been proposed for celecoxib-induced increases in $[Ca^{2+}]_i$ such as the inhibition of SERCA, permeabiliza-

Please cite this article in press as: Ishihara T, et al. Protective effect of rebamipide against celecoxib-induced gastric mucosal cell apoptosis. Biochem Pharmacol (2010), doi:10.1016/j.bcp.2010.01.030

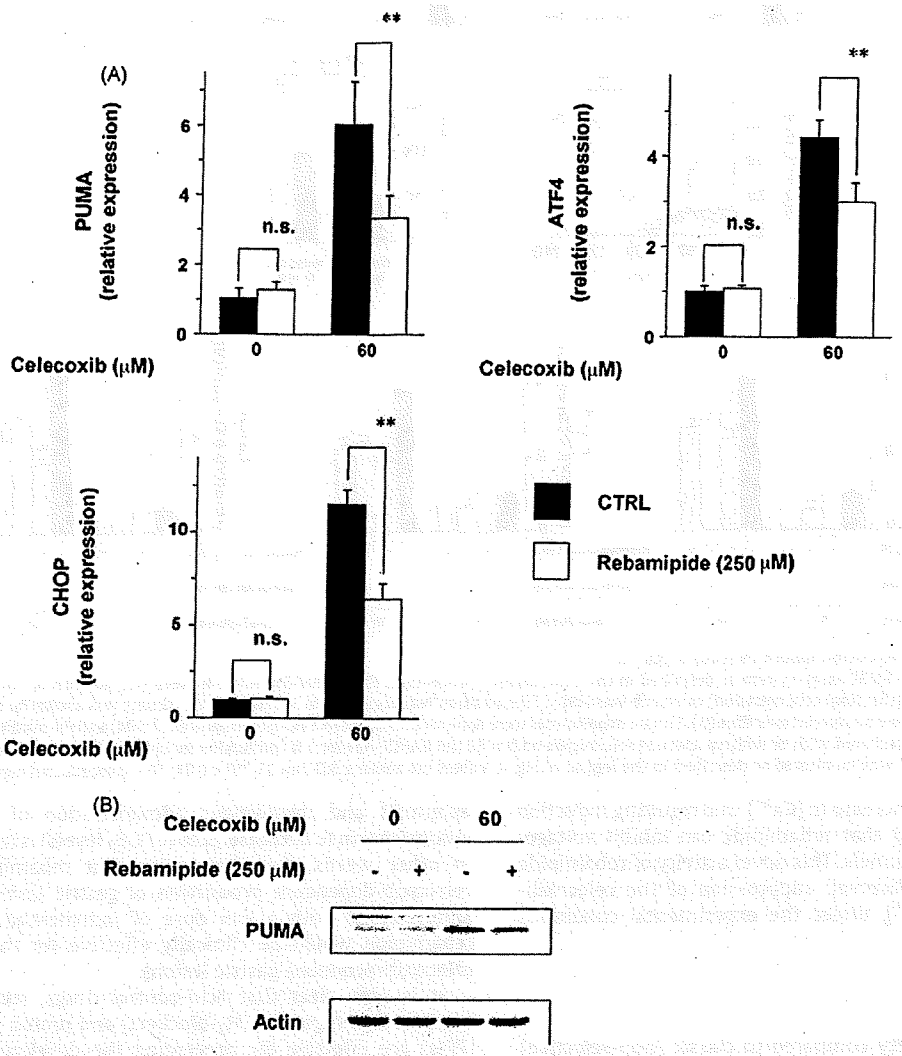

Fig. 4. Effect of rebamipide on the celecoxib-induced ER stress response.
AGS cells were incubated with or without (CTRL) 250 μM rebamipide for 1 h and further incubated with or without 60 μM celecoxib for 12 h (A) or 18 h (B). The relative expression of each gene was monitored by real-time RT-PCR using specific primers for each gene. Values normalized to the *actin* gene are expressed relative to the control sample. Values are mean ± S.D. ($n = 3$). $^{**}P < 0.01$; n.s., not significant (A). Whole cell lysates were analysed by immunoblotting with an antibody against *puma* or actin (B).

tion of cytoplasmic membranes and activation of voltage-dependent L-type Ca^{2+} channels [17,41,42]. It seems that the mechanism involved depends on the cell species and culture conditions. To address this issue, we monitored $[Ca^{2+}]_i$ under Ca^{2+}-free conditions. As shown in Fig. 7A, a celecoxib-induced increase in $[Ca^{2+}]_i$ was not observed under Ca^{2+}-free conditions, suggesting that most of the increase is derived from extracellular Ca^{2+} and not from Ca^{2+} in intracellular compartments (such as the ER). The involvement of SERCA in celecoxib-induced increases in $[Ca^{2+}]_i$ under the experimental conditions was not supported by the observation that rebamipide did not affect the thapsigargin-induced increase in $[Ca^{2+}]_i$ (Fig. 6A). We previously established an assay system for measuring the membrane permeabilization activity of NSAIDs, using calcein-loaded liposomes. Calcein fluorescence is very weak at high concentrations due to self-quenching, so the addition of membrane-permeabilizing drugs to a medium containing calcein-loaded liposomes causes an increase in fluorescence by diluting the calcein [17,19,36]. We confirmed that celecoxib increases calcein fluorescence (data not shown). We then examined the effect of rebamipide on the celecoxib-dependent increase in calcein fluorescence. The addition of rebamipide (up to 1000 μM) to the medium did not affect the celecoxib-dependent increase in calcein fluorescence (Fig. 7B). We have previously monitored celecoxib-dependent permeabilization of cytoplasmic membranes by monitoring K^+ efflux from cells [17,36]. The K^+ concentration in the culture medium increased in the presence of celecoxib (60–400 μM), showing that K^+ efflux from AGS cells was stimulated, and rebamipide (250 μM) did not affect this increase (Fig. 7C). The results shown in Fig. 7B and C suggest that rebamipide did not affect celecoxib-dependent membrane permeabilization and that, under the experimental conditions used, permeabilization of cytoplasmic membranes is not involved in celecoxib-induced increases in $[Ca^{2+}]_i$.

Next, we examined the effect of nifedipine, an inhibitor of voltage-dependent L-type Ca^{2+} channels, on celecoxib (60 μM)-induced increases in $[Ca^{2+}]_i$ and found that nifedipine (10 μM) suppresses this increase (Fig. 7D). We also found that not only nifedipine but also rebamipide (250 μM) suppressed the increase in $[Ca^{2+}]_i$ induced by BAY K 8644 (3 μM), an activator of voltage-dependent L-type Ca^{2+} channels (Fig. 7E). Celecoxib-induced expression of ER stress response-related genes was also suppressed by nifedipine (10 μM) (Fig. 7F). These results suggest that, under the experimental conditions used, activation of voltage-dependent L-type Ca^{2+} channels is the main mechanism involved

Please cite this article in press as: Ishihara T, et al. Protective effect of rebamipide against celecoxib-induced gastric mucosal cell apoptosis. Biochem Pharmacol (2010), doi:10.1016/j.bcp.2010.01.030

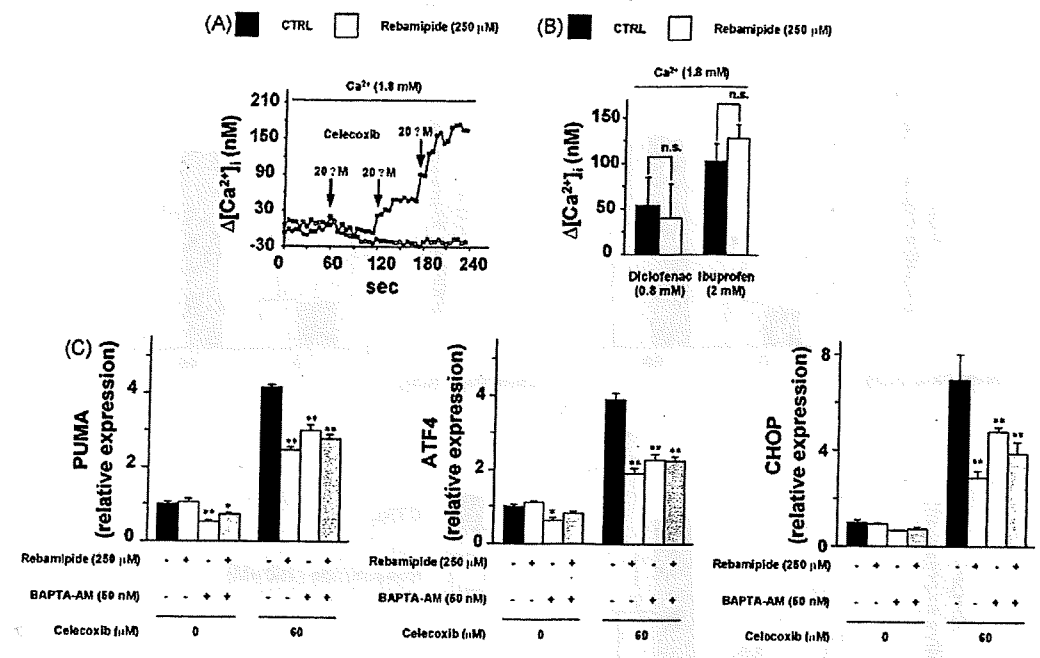

Fig. 5. Effect of rebamipide on celecoxib-induced increase in $[Ca^{2+}]_i$.
$[Ca^{2+}]_i$ was monitored by a fluo-3/AM assay system as described in the experimental procedures. Fluo-3/AM-loaded cells were treated with or without (CTRL) 250 μM rebamipide for 10 min, then 60 μM (final concentration) celecoxib was added (the addition was divided into 3 times and the timing was shown by arrows in figure) and changes in fluo-3 fluorescence were monitored over time (A). Similar experiments were done for diclofenac (0.8 mM) or ibuprofen (2 mM) and the maximum values for $[Ca^{2+}]_i$ are shown (B). AGS cells were incubated with or without 250 μM rebamipide and/or 50 nM BAPTA-AM for 1 h and further incubated with 60 μM celecoxib for 12 h. The relative expression of each gene was monitored as described in the legend of Fig. 4. Values are mean ± S.D. ($n = 3$). $^{**}P < 0.01$; $^{*}P < 0.05$; n.s., not significant (C).

in the celecoxib-induced increase in $[Ca^{2+}]_i$ and resulting induction of ER stress response and that rebamipide can inhibit voltage-dependent L-type Ca^{2+} channels. This novel activity of rebamipide would account for the observed suppression of the celecoxib-induced increase in $[Ca^{2+}]_i$ under the experimental conditions used.

4. Discussion

Due to its relative safety compared to classic (non-selective) NSAIDs, celecoxib is used widely in Western countries. However, this drug has only very recently become available in Japan. Rebamipide, while not used in Western countries, is a leading anti-ulcer drug in the Japanese market and it has therefore recently come into use in Japan for the prevention of celecoxib-induced gastric lesions. It is important then that the effect of rebamipide on celecoxib-induced gastric lesions be examined in both humans and animals. In this study, for the first time, we have shown that rebamipide suppresses celecoxib-dependent production of gastric lesions in animals and have examined the molecular mechanism by which it has this effect (see below).

Although oral administration of celecoxib produces significant levels of gastric lesions in humans, especially upon long-term treatment or in patients co-administered with low doses of aspirin [10,13,14], it produces few gastric lesions in animals [39]. We recently proposed that both a decrease in the gastric PGE_2 level and gastric mucosal apoptosis are required for the formation of NSAID-induced gastric lesions *in vivo* [21,25,26]. Based on this idea, we consider that celecoxib does not produce acute gastric lesions in animals due to its inability to decrease the gastric PGE_2 level and that an accidental (celecoxib-independent) decrease in gastric PGE_2 level or that induced by a low dose of aspirin causes the observed celecoxib-dependent production of gastric lesions in humans (celecoxib has strong apoptosis-inducing activity [19]). Therefore, we consider that the model that we used in this study (oral administration of celecoxib to induce gastric mucosal apoptosis and intravenous administration of a low dose of indomethacin to decrease gastric PGE_2 levels) is relevant clinically. In other words, the observation that rebamipide suppresses celecoxib-dependent production of gastric lesions in mice pre-administered with a low dose of indomethacin suggests that rebamipide would be clinically effective for the prevention of celecoxib-produced gastric lesions.

It is now clear that acid-control drugs, such as histamine receptor-2 antagonists (H_2-blockers) and proton pump inhibitors (PPIs) are effective for preventing the development of NSAID-induced gastric lesions in Western countries [43]. However, since gastric acid secretion in Asian populations is much lower than in Western populations [28,44,45], acid-control drugs may not be so effective for Asian populations. In fact, it was reported that the efficacy of rebamipide for prevention of NSAID-induced gastric ulcers is much the same as that of famotidine, an H_2-blocker in Japanese populations [30]. Thus, anti-ulcer drugs other than acid-control drugs (such as rebamipide) may be particularly important in Asian countries.

In our mouse model (in which celecoxib and indomethacin were co-administered), oral administration of rebamipide suppressed gastric mucosal apoptosis but did not affect the decrease in the gastric PGE_2 level. It has previously been reported that rebamipide increases gastric PGE_2 levels by up-regulation of expression of COX-2 [33,46]. This discrepancy may be explained by differences in the rebamipide treatment: they administered rebamipide for 14 days (once per day) to detect up-regulation of expression of COX-2 and an increase in the gastric PGE_2 level [46].

We have previously suggested that celecoxib-induced apoptosis is mediated by an increase in $[Ca^{2+}]_i$, induction of the ER stress response, activation and translocation of Bax, mitochondrial dysfunction and activation of caspases [17,22–24]. It is possible that induction of the ER stress response by increase in $[Ca^{2+}]_i$ is mediated by Ca^{2+}-induced Ca^{2+}-release and resulting depletion of Ca^{2+} level in ER; Ca^{2+} channels on ER membrane (inositol-1,4,5-triphosphate receptor and ryanodine receptor) that are involved in

Please cite this article in press as: Ishihara T, et al. Protective effect of rebamipide against celecoxib-induced gastric mucosal cell apoptosis. Biochem Pharmacol (2010), doi:10.1016/j.bcp.2010.01.030

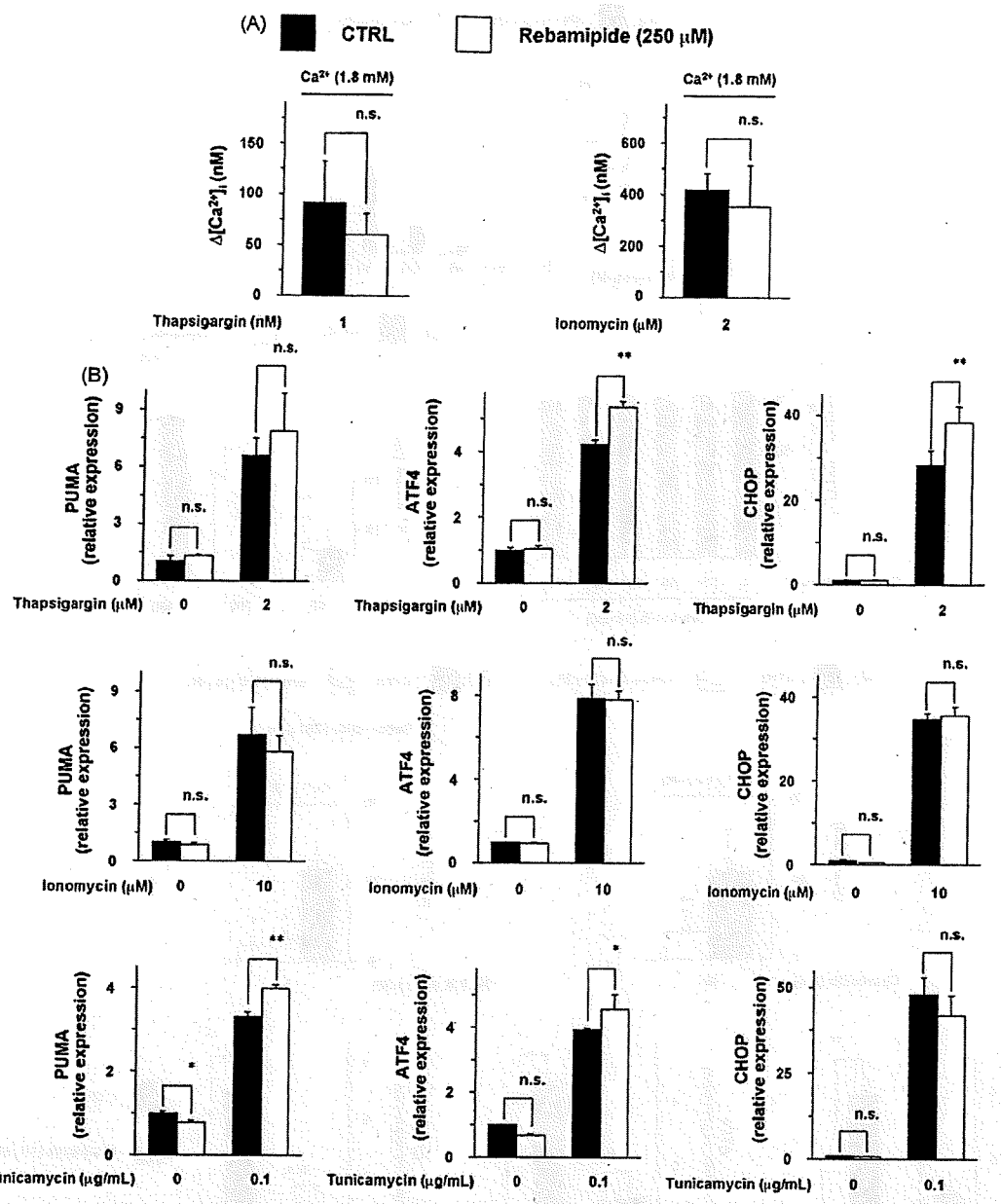

Fig. 6. Effect of rebamipide on the increase in $[Ca^{2+}]_i$ and ER stress response induced by other chemicals.
The effect of 250 μM rebamipide on increases in $[Ca^{2+}]_i$ ($\Delta[Ca^{2+}]_i$) (A) and the ER stress response (B) in the presence of the indicated concentrations of thapsigargin, ionomycin and tunicamycin was monitored as described in the legends of Figs. 4 and 5. Values are mean ± S.D. ($n = 3$). $^{**}P < 0.01$; $^{*}P < 0.05$; n.s., not significant (A, B).

Ca^{2+}-release in ER, are activated by increase in $[Ca^{2+}]_i$ [47]. Here, we have found that all of these steps are suppressed by rebamipide, suggesting that rebamipide protects cells against celecoxib-induced apoptosis through maintenance of $[Ca^{2+}]_i$. Of the various proposed mechanisms for the celecoxib-induced increase in $[Ca^{2+}]_i$ (inhibition of SERCA, permeabilization of cytoplasmic membranes and activation of voltage-dependent L-type Ca^{2+} channels), we suggest that, under the experimental conditions used, activation of voltage-dependent L-type Ca^{2+} channels is mainly responsible for the celecoxib-induced increase in $[Ca^{2+}]_i$ and that rebamipide suppresses this activation. This conclusion is based on the following observations: (i) rebamipide suppressed the increase in $[Ca^{2+}]_i$ induced by BAY K 8644 but not by thapsigargin, (ii) rebamipide did not affect celecoxib-induced membrane permeabilization, (iii) nifedipine suppressed the increase in $[Ca^{2+}]_i$ induced by celecoxib. Anti-apoptotic effects of voltage-dependent L-type Ca^{2+} channel inhibitors have also been reported for renal tubular cells and colon cells [48,49]. The finding that rebamipide can block this type of Ca^{2+} channel is novel and this property may be responsible for various pharmacological activities of this drug. For example, it has been reported that rebamipide suppresses activation of neutrophils through suppressing an increase in $[Ca^{2+}]_i$ and that this activity of rebamipide plays an important role in conferring protection against NSAID-induced gastric lesions [50,51]. Our results suggest that this effect of rebamipide is mediated by inhibition of voltage-dependent L-type Ca^{2+} channels, because these Ca^{2+} channels have been suggested to be involved in the activation of neutrophils and their adhesion to fibrinogen [52,53]. Since increases in $[Ca^{2+}]_i$ play an important role in the production of ROS [52,53], it is also possible that this novel activity of rebamipide is involved in its well-known ROS-decreasing activity. It has been reported that inhibition of voltage-dependent

Please cite this article in press as: Ishihara T, et al. Protective effect of rebamipide against celecoxib-induced gastric mucosal cell apoptosis. Biochem Pharmacol (2010), doi:10.1016/j.bcp.2010.01.030

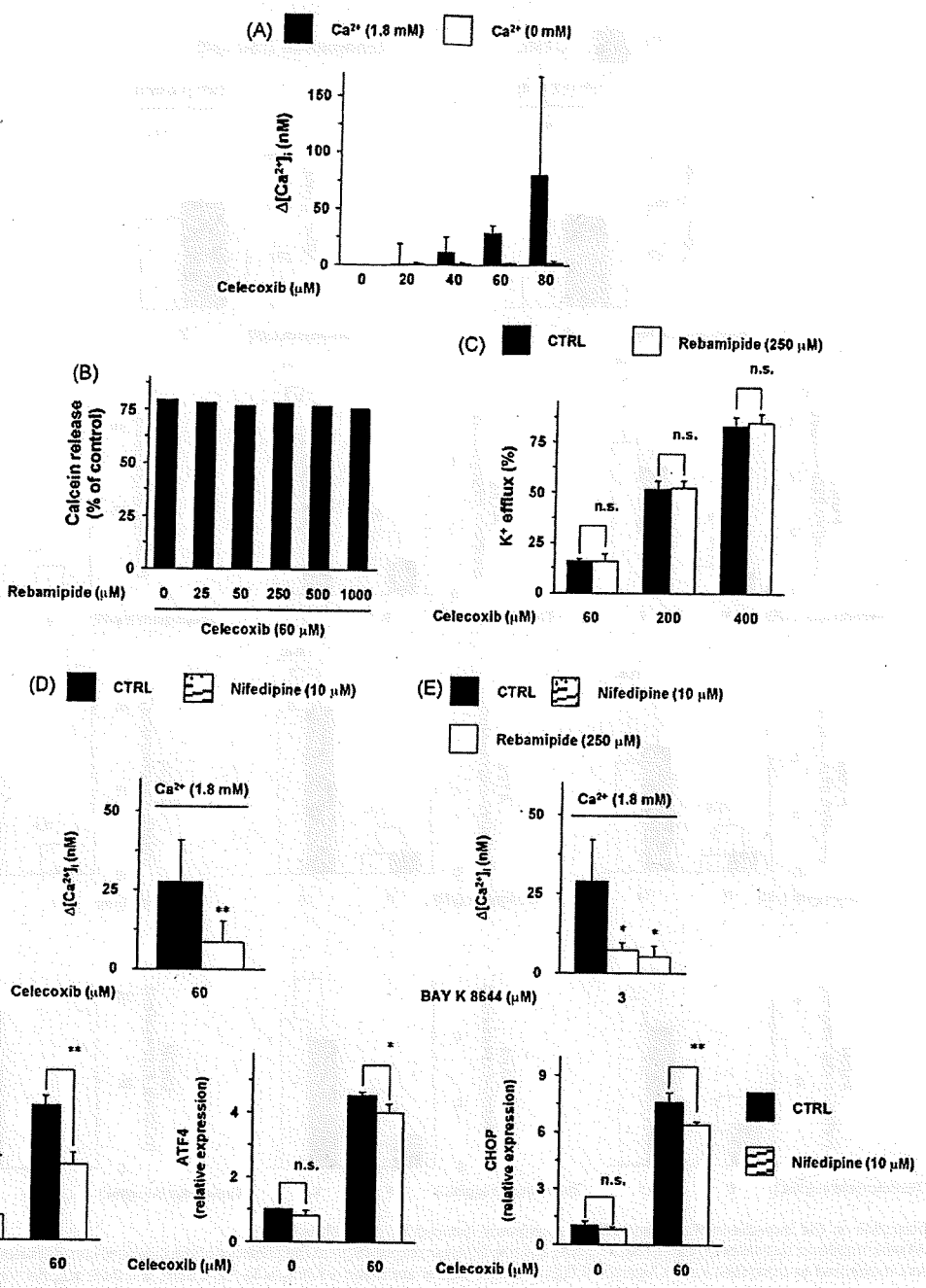

Fig. 7. Mechanism for rebamipide-dependent suppression of the celecoxib-induced increase in $[Ca^{2+}]_i$.
The effect of the indicated concentrations of celecoxib on the increase in $[Ca^{2+}]_i$ ($\Delta[Ca^{2+}]_i$) under Ca^{2+}-containing (+) or Ca^{2+}-free (-) conditions was monitored as described in the legend of Fig. 5 (A). Calcein-loaded liposomes were pre-incubated for 10 min with the indicated concentration of rebamipide and further incubated for 10 min with or without 60 μM celecoxib in the presence of the same concentration of rebamipide as was used in the pre-incubation step. The release of calcein from liposomes was determined by measuring fluorescence intensity. Triton X-100 (10 μl/ml) was used to determine the 100% level of membrane permeabilization (B). AGS cells were incubated with or without (CTRL) 250 μM rebamipide for 1 h and further incubated with the indicated concentrations of celecoxib for 10 min and the level of K^+ efflux was measured using a K^+ ion-selective electrode. Melittin (10 μM) was used to establish the 100% level of K^+ efflux (C). The effects of nifedipine (10 μM) (D-F) or rebamipide (250 μM) (E) on celecoxib – (D) or BAY K 8644 – (E) induced increases in $[Ca^{2+}]_i$ ($\Delta[Ca^{2+}]_i$) (D, E) or celecoxib-induced ER stress response (F) were monitored as described in the legend of Fig. 4 (D–F). Cells were pre-incubated with nifedipine for 1 h and further incubated with celecoxib without nifedipine for 12 h (F). Values are mean ± S.D. ($n = 3$). $^{**}P < 0.01$; $^{*}P < 0.05$; n.s., not significant (A, C–F).

L-type Ca^{2+} channels suppresses gastrin-induced histamine release from gastric enterochromaffin-like cells [54], suggesting that some part of the gastroprotective effect of rebamipide is mediated by suppression of gastrin-induced histamine release through its inhibitory effect on voltage-dependent L-type Ca^{2+} channels. Furthermore, since inhibition of voltage-dependent L-type Ca^{2+} channels was suggested to have beneficial effects on various disorders, such as immune disorders [55], the results of this study suggest that rebamipide has some beneficial effects on these disorders through its inhibitory effect on voltage-dependent L-type Ca^{2+} channels.

In conclusion, we have found that rebamipide has a novel activity, inhibition of the voltage-dependent L-type Ca^{2+} channels, and suggest that this activity is involved in rebamipide-dependent

Please cite this article in press as: Ishihara T, et al. Protective effect of rebamipide against celecoxib-induced gastric mucosal cell apoptosis. Biochem Pharmacol (2010), doi:10.1016/j.bcp.2010.01.030

protection of cells against celecoxib-induced apoptosis *in vitro* and protection of gastric mucosa against production of lesions *in vivo*. This finding is important in understanding the mechanism whereby this drug has its gastroprotective effects and may prove useful in expanding the clinical application of this drug to include other diseases.

Acknowledgements

This work was supported by Grants-in-Aid of Scientific Research from the Ministry of Health, Labour, and Welfare of Japan, Grants-in-Aid for Scientific Research from the Ministry of Education, Culture, Sports, Science and Technology of Japan, and Grants-in-Aid of the Japan Science and Technology Agency.

References

[1] Smalley WE, Ray WA, Daugherty JR, Griffin MR. Non-steroidal anti-inflammatory drugs and the incidence of hospitalizations for peptic ulcer disease in elderly persons. Am J Epidemiol 1995;141:539–45.
[2] Hawkey CJ. Non-steroidal anti-inflammatory drug gastropathy. Gastroenterology 2000;119:521–35.
[3] Barrier CH, Hirschowitz BI. Controversies in the detection and management of non-steroidal antiinflammatory drug-induced side effects of the upper gastrointestinal tract. Arthritis Rheum 1989;32:926–32.
[4] Fries JF, Miller SR, Spitz PW, Williams CA, Hubert HB, Bloch DA. Toward an epidemiology of gastropathy associated with non-steroidal antiinflammatory drug use. Gastroenterology 1989;96:647–55.
[5] Gabriel SE, Jaakkimainen L, Bombardier C. Risk for serious gastrointestinal complications related to use of non-steroidal anti-inflammatory drugs. A meta-analysis. Ann Intern Med 1991;115:787–96.
[6] Kurata JH, Abbey DE. The effect of chronic aspirin use on duodenal and gastric ulcer hospitalizations. J Clin Gastroenterol 1990;12:260–6.
[7] Vane J. Towards a better aspirin. Nature 1994;367:215–6.
[8] Smith CJ, Zhang Y, Koboldt CM, Muhammad J, Zweifel BS, Shaffer A, et al. Pharmacological analysis of cyclooxygenase-1 in inflammation. Proc Natl Acad Sci U S A 1998;95:13313–8.
[9] Chan CC, Boyce S, Brideau C, Charleson S, Cromlish W, Ethier D, et al. Rofecoxib [Vioxx, MK-0966; 4-(4′-methylsulfonylphenyl)-3-phenyl-2-(5H)-furanone]: a potent and orally active cyclooxygenase-2 inhibitor. Pharmacological and biochemical profiles. J Pharmacol Exp Ther 1999;290:551–60.
[10] Silverstein FE, Faich G, Goldstein JL, Simon LS, Pincus T, Whelton A, et al. Gastrointestinal toxicity with celecoxib vs. non-steroidal anti-inflammatory drugs for osteoarthritis and rheumatoid arthritis: the CLASS study: A randomized controlled trial. Celecoxib Long-term Arthritis Safety Study. J Am Med Assoc 2000;284:1247–55.
[11] Bombardier C, Laine L, Reicin A, Shapiro D, Burgos VR, Davis B, et al. Comparison of upper gastrointestinal toxicity of rofecoxib and naproxen in patients with rheumatoid arthritis. VIGOR Study Group. N Engl J Med 2000;343:1520–8. 2 p following 8.
[12] FitzGerald GA, Patrono C. The coxibs, selective inhibitors of cyclooxygenase-2. N Engl J Med 2001;345:433–42.
[13] Juni P, Rutjes AW, Dieppe PA. Are selective COX 2 inhibitors superior to traditional non-steroidal anti-inflammatory drugs? Br Med J 2002;324:1287–8.
[14] Lanas A, Garcia-Rodriguez LA, Arroyo MT, Gomollon F, Feu F, Gonzalez-Perez A, et al. Risk of upper gastrointestinal ulcer bleeding associated with selective cyclooxygenase-2 inhibitors, traditional non-aspirin non-steroidal anti-inflammatory drugs, aspirin and combinations. Gut 2006;55:1731–8.
[15] Vane JR, Botting RM. Mechanism of action of anti-inflammatory drugs. Scand J Rheumatol Suppl 1996;102:9–21.
[16] Miller TA. Protective effects of prostaglandins against gastric mucosal damage: current knowledge and proposed mechanisms. Am J Physiol 1983;245: G601–23.
[17] Tanaka K, Tomisato W, Hoshino T, Ishihara T, Namba T, Aburaya M, et al. Involvement of Intracellular Ca2+ Levels in non-steroidal anti-inflammatory drug-induced apoptosis. J Biol Chem 2005;280:31059–67.
[18] Tsutsumi S, Gotoh T, Tomisato W, Mima S, Hoshino T, Hwang HJ, et al. Endoplasmic reticulum stress response is involved in non-steroidal anti-inflammatory drug-induced apoptosis. Cell Death Differ 2004;11:1009–16.
[19] Tomisato W, Tanaka K, Katsu T, Kakuta H, Sasaki K, Tsutsumi S, et al. Membrane permeabilization by non-steroidal anti-inflammatory drugs. Biochem Biophys Res Commun 2004;323:1032–9.
[20] Tomisato W, Tsutsumi S, Rokutan K, Tsuchiya T, Mizushima T. NSAIDs induce both necrosis and apoptosis in guinea pig gastric mucosal cells in primary culture. Am J Physiol Gastrointest Liver Physiol 2001;281:G1092–100.
[21] Aburaya M, Tanaka K, Hoshino T, Tsutsumi S, Suzuki K, Makise M, et al. Heme oxygenase-1 protects gastric mucosal cells against non-steroidal anti-inflammatory drugs. J Biol Chem 2006;281:33422–3.
[22] Ishihara T, Hoshino T, Namba T, Tanaka K, Mizushima T. Involvement of up-regulation of *puma* in non-steroidal anti-inflammatory drug-induced apoptosis. Biochem Biophys Res Commun 2007;356:711–7.
[23] Tsutsumi S, Namba T, Tanaka KI, Arai Y, Ishihara T, Aburaya M, et al. Celecoxib upregulates endoplasmic reticulum chaperones that inhibit celecoxib-induced apoptosis in human gastric cells. Oncogene 2006;25: 1018–29.
[24] Namba T, Hoshino T, Tanaka K, Tsutsumi S, Ishihara T, Mima S, et al. Up-regulation of 150-kDa oxygen-regulated protein by celecoxib in human gastric carcinoma cells. Mol Pharmacol 2007;71:860–70.
[25] Tomisato W, Tsutsumi S, Hoshino T, Hwang HJ, Mio M, Tsuchiya T, et al. Role of direct cytotoxic effects of NSAIDs in the induction of gastric lesions. Biochem Pharmacol 2004;67:575–85.
[26] Suemasu S, Tanaka K, Namba T, Ishihara T, Katsu T, Fujimoto M, et al. A role for HSP70 in protecting against indomethacin-induced gastric lesions. J Biol Chem 2009;284:19705–1.
[27] Arakawa T, Higuchi K, Fujiwara Y, Watanabe T, Tominaga K, Sasaki E, et al. 15th anniversary of rebamipide: looking ahead to the new mechanisms and new applications. Dig Dis Sci 2005;50(Suppl 1):S3–11.
[28] Haruma K, Ito M. Review article: clinical significance of mucosal-protective agents: acid, inflammation, carcinogenesis and rebamipide. Aliment Pharmacol Ther 2003;18(Suppl. 1):153–9.
[29] Hiratsuka T, Futagami S, Shindo T, Hamamoto T, Ueki N, Suzuki K, et al. Rebamipide reduces indomethacin-induced gastric injury in mice via down-regulation of ICAM-1 expression. Dig Dis Sci 2005;50(Suppl. 1):S84–9.
[30] Naito Y, Iinuma S, Yagi N, Boku Y, Imamoto E, Takagi T, et al. Prevention of indomethacin-induced gastric mucosal injury in helicobacter pylori-negative healthy volunteers: A comparison study rebamipide vs. famotidine. J Clin Biochem Nutr 2008;43:34–40.
[31] Kleine A, Kluge S, Peskar BM. Stimulation of prostaglandin biosynthesis mediates gastroprotective effect of rebamipide in rats. Dig Dis Sci 1993;38:1441–9.
[32] Yoshikawa T, Naito Y, Tanigawa T, Kondo M. Free radical scavenging activity of the novel anti-ulcer agent rebamipide studied by electron spin resonance. Arzneimittelforschung 1993;43:363–6.
[33] Murata H, Yabe Y, Tsuji S, Tsujii M, Fu HY, Asahi K, et al. Gastro-protective agent rebamipide induces cyclooxygenease-2 (COX-2) in gastric epithelial cells. Dig Dis Sci 2005;50(Suppl 1):S70–5.
[34] Nagano Y, Matsui H, Muramatsu M, Shimokawa O, Shibahara T, Yanaka A, et al. Rebamipide significantly inhibits indomethacin-induced mitochondrial damage, lipid peroxidation, and apoptosis in gastric epithelial RGM-1 cells. Dig Dis Sci 2005;50(Suppl. 1):S76–83.
[35] Naito Y, Kajikawa H, Mizushima K, Shimozawa M, Kuroda M, Katada K, et al. Rebamipide, a gastro-protective drug, inhibits indomethacin-induced apoptosis in cultured rat gastric mucosal cells: association with the inhibition of growth arrest and DNA damage-induced 45 alpha expression. Dig Dis Sci 2005;50(Suppl. 1):S104–12.
[36] Ushijima H, Tanaka K, Takeda M, Katsu T, Mima S, Mizushima T. Geranylgeranylacetone protects membranes against non-steroidal anti-inflammatory drugs. Mol Pharmacol 2005;68:1156–61.
[37] Tsutsumi S, Tomisato W, Takano T, Rokutan K, Tsuchiya T, Mizushima T. Gastric irritant-induced apoptosis in guinea pig gastric mucosal cells in primary culture. Biochim Biophys Acta 2002;1589:168–80.
[38] Bradford MM. A rapid and sensitive method for the quantitation of microgram quantities of protein utilizing the principle of protein-dye binding. Anal Biochem 1976;72:248–54.
[39] Laudanno OM, Cesolari JA, Esnarriaga J, Rista L, Piombo G, Maglione C, et al. Gastrointestinal damage induced by celecoxib and rofecoxib in rats. Dig Dis Sci 2001;46:779–84.
[40] Makin GW, Corfe BM, Griffiths GJ, Thistlethwaite A, Hickman JA, Dive C. Damage-induced Bax N-terminal change, translocation to mitochondria and formation of Bax dimers/complexes occur regardless of cell fate. Embo J 2001;20:6306–15.
[41] Johnson AJ, Hsu AL, Lin HP, Song X, Chen CS. The cyclooxygenase-2 inhibitor celecoxib perturbs intracellular calcium by inhibiting endoplasmic reticulum Ca2+-ATPases: a plausible link with its anti-tumour effect and cardiovascular risks. Biochem J 2002;366:831–7.
[42] Wang JL, Lin KL, Chen JS, Lu YC, Jiann BP, Chang HT, et al. Effect of celecoxib on Ca2+ movement and cell proliferation in human osteoblasts. Biochem Pharmacol 2004;67:1123–30.
[43] Moore RA, Derry S, Phillips CJ, McQuay HJ. Non-steroidal anti-inflammatory drugs (NSAIDs), cyclooxygenase-2 selective inhibitors (coxibs) and gastrointestinal harm: review of clinical trials and clinical practice. BMC Musculoskelet Disord 2006;7:79.
[44] Lam SK, Hasan M, Sircus W, Wong J, Ong GB, Prescott RJ. Comparison of maximal acid output and gastrin response to meals in Chinese and Scottish normal and duodenal ulcer subjects. Gut 1980;21:324–8.
[45] Cheng FC, Lam SK, Ong GB. Maximum acid output to graded doses of pentagastrin and its relation to parietal cell mass in Chinese patients with duodenal ulcer. Gut 1977;18:827–32.
[46] Sun WH, Tsuji S, Tsujii M, Gunawan ES, Kawai N, Kimura A, et al. Induction of cyclooxygenase-2 in rat gastric mucosa by rebamipide, a mucoprotective agent. J Pharmacol Exp Ther 2000;295:447–52.
[47] Berridge MJ, Lipp P, Bootman MD. The versatility and universality of calcium signalling. Nat Rev Mol Cell Biol 2000;1:11–21.
[48] Tanaka T, Nangaku M, Miyata T, Inagi R, Ohse T, Ingelfinger JR, et al. Blockade of calcium influx through L-type calcium channels attenuates mitochondrial injury and apoptosis in hypoxic renal tubular cells. J Am Soc Nephrol 2004;15:2320–33.

Please cite this article in press as: Ishihara T, et al. Protective effect of rebamipide against celecoxib-induced gastric mucosal cell apoptosis. Biochem Pharmacol (2010), doi:10.1016/j.bcp.2010.01.030

THE JOURNAL OF BIOLOGICAL CHEMISTRY VOL. 285, NO. ??, pp. 1–xxx, ???? ??, 2010

Suppression of Melanin Production by Expression of HSP70*[S]

Received for publication, January 11, 2010, and in revised form, February 14, 2010 Published, JBC Papers in Press, February 22, 2010, DOI 10.1074/jbc.M110.103051

Tatsuya Hoshino[‡], Minoru Matsuda[‡], Yasuhiro Yamashita[‡], Masaya Takehara[‡], Masayo Fukuya[‡], Kazutaka Mineda[§], Daisuke Maji[§], Hironobu Ihn[‡], Hiroaki Adachi[¶], Gen Sobue[¶], Yoko Funasaka[‖], and Tohru Mizushima[‡1]

From the [‡]Graduate School of Medical and Pharmaceutical Sciences, Kumamoto University, Kumamoto 862-0973, [§]Saishunkan Pharmaceutical Co. Ltd, Kumamoto 861-2201, the [¶]Nagoya University Graduate School of Medicine, Nagoya 466-8550, and the [‖]Kobe University Graduate School of Medicine, Kobe 650-0017, Japan

Skin hyperpigmentation disorders due to abnormal melanin production induced by ultraviolet (UV) irradiation are both a clinical and cosmetic problem. UV irradiation stimulates melanin production in melanocytes by increasing intracellular cAMP. Expression of heat shock proteins (HSPs), especially HSP70, is induced by various stressors, including UV irradiation, to provide cellular resistance to such stressors. In this study we examined the effect of expression of HSP70 on melanin production both *in vitro* and *in vivo*. 3-Isobutyl-1-methylxanthine (IBMX), a cAMP-elevating agent, stimulated melanin production in cultured mouse melanoma cells, and this stimulation was suppressed in cells overexpressing HSP70. IBMX-dependent transcriptional activation of the tyrosinase gene was also suppressed in HSP70-overexpressing cells. Expression of microphthalmia-associated transcription factor (MITF), which positively regulates transcription of the tyrosinase gene, was up-regulated by IBMX; however, this up-regulation was not suppressed in HSP70-overexpressing cells. On the other hand, immunoprecipitation and immunostaining analyses revealed a physical interaction between and co-localization of MITF and HSP70, respectively. Furthermore, the transcription of tyrosinase gene in nuclear extract was inhibited by HSP70. *In vivo*, UV irradiation of wild-type mice increased the amount of melanin in the basal layer of the epidermis, and this increase was suppressed in transgenic mice expressing HSP70. This study provides the first evidence of an inhibitory effect of HSP70 on melanin production both *in vitro* and *in vivo*. This effect seems to be mediated by modulation of MITF activity through a direct interaction between HSP70 and MITF.

The skin can structurally be divided into several layers including the most apical layer, the epidermis, consisting of keratinocytes (1). In addition to changes with aging, the skin is damaged by various environmental stressors, especially by solar ultraviolet irradiation (photo-aging). UV light can be separated, based on the wavelength, into UVA (320–400 nm), UVB (290–320 nm), and UVC (100–290 nm) (2). Of these, most UVC can be absorbed by the ozone layer. Although the cell-damaging effect of UVA is relatively weak, UVA seems to play an important role in photo-aging because its content in solar UV is higher than UVB and UVC (3–5). Furthermore, UVB seems to also play the central role in photo-aging (6).

UV-induced skin hyperpigmentation disorders due to abnormal melanin production cause clinical and cosmetic problems. UV-dependent delayed pigmentation (induction of melanin production and distribution) plays a central role in the hyperpigmentation disorders. The induction of melanin production is mediated by various signal pathways (7–9). Of these pathways, a cAMP-dependent pathway seems to play a central role in UV-dependent stimulation of melanin production (7). In this pathway, exposure of keratinocytes to UV stimulates the release of signal molecules, such as α-melanocyte-stimulating hormone (α-MSH),[2] prostaglandin E_2, adenocorticotropic hormone, and endotheline-1, all of which stimulate melanin production in melanocytes through elevation of the level of intracellular cAMP. For example, the binding of α-MSH or adenocorticotropic hormone to melanocortin 1 receptor on melanocytes induces the expression of tyrosinase and other melanogenesis-related proteins through activation of adenylate cyclase, an increase in the intracellular cAMP level, activation of protein kinase A, activation of the cAMP response element-binding protein (CREB), and induction of expression of microphthalmia-associated transcription factor (MITF) that specifically binds to the promoter of the tyrosinase gene to promote its transcription (7). Tyrosinase is a rate-limiting enzyme in melanin synthesis, and an increase in the activity and expression of tyrosinase was observed in sites of UV-induced hyperpigmentation (10, 11); therefore, chemicals and natural products that suppress the activity and/or expression of tyrosinase could be pharmaceutically and cosmetically beneficial as hypopigmenting agents.

On the other hand, UV-induced modest melanin production plays an important role in protection of the skin against UV-dependent damage, including DNA damage (12). This protection is particularly important for the prevention of UV-induced development of melanoma and non-melanoma skin cancer

* This work was supported by grants-in-aid for Scientific Research from the Ministry of Health, Labour, and Welfare of Japan as well as the Japan Science and Technology Agency and grants-in-aid for Scientific Research from the Ministry of Education, Culture, Sports, Science, and Technology, Japan.

[S] The on-line version of this article (available at http://www.jbc.org) contains supplemental Figs. S1–S4.

[1] To whom correspondence should be addressed: Graduate School of Medical and Pharmaceutical Sciences, Kumamoto University, 5-1 Oe-honmachi, Kumamoto 862-0973, Japan. Tel. and Fax: 81-96-371-4323; E-mail: mizu@gpo.kumamoto-u.ac.jp.

[2] The abbreviations used are: α-MSH, α-melanocyte-stimulating hormone; ERK, extracellular signal-regulated kinase; GAPDH, glyceraldehyde-3-phosphate dehydrogenase; GRP, glucose-regulated protein; HSP, heat shock protein; IBMX, 3-isobutyl-1-methylxanthine; MITF, microphthalmia-associated transcription factor; p38 MAPK, p38 mitogen-activated protein kinase; siRNA, small interfering RNA; RT, reverse transcription; GST, glutathione *S*-transferase.

294

balt3/zbc-bc/zbc-bc/zbc02010/zbc1371-10z ZSUBMIT 32 xppws S=1 9/3/10 5:24 4/Color Figure(s) F5,8 ARTNO: M110.103051

(13). Synthesized melanin in the melanosomes in melanocytes is distributed and transported to the surrounding keratinocytes where it forms a melanin cap that acts as a filter to limit the penetration of UV into the epidermis and dermis (14). Melanin also acts as a scavenger of UV-produced reactive oxygen species that are also responsible for UV-dependent skin damage and development of skin cancer (15). Thus, identification of a mechanism that not only suppresses melanin production but also protects the skin from UV-induced damage is important for developing hypopigmenting agents (skin whitening agents) without worsening UV-induced skin damage.

When cells are exposed to stressors, a number of so-called stress proteins are induced to confer protection against such stressors. HSPs are representative of these stress proteins, and their cellular up-regulation of expression, especially that of HSP70, provides resistance as the HSPs re-fold or degrade denatured proteins produced by stressors such as reactive oxygen species (16). Because stressor-induced tissue damage is involved in various diseases, HSPs and HSP inducers have received much attention for their therapeutic potential. For example, we have shown using transgenic mice that HSP70 protects the gastrointestinal tract from development of gastric and small intestinal lesions and inflammatory bowel disease (17–20). Interestingly, geranylgeranylacetone, a leading anti-ulcer drug on the Japanese market, has been reported to be a non-toxic HSP-inducer, up-regulating various HSPs not only in cultured gastric mucosal cells but also in various tissues, including the gastric mucosa *in vivo* (21). It was recently reported that geranylgeranylacetone suppresses inflammatory bowel disease-related experimental colitis and lesion of small intestine (19, 22, 23). Based on these results, it is expected that non-toxic HSP inducers, including geranylgeranylacetone, will be therapeutically beneficial for various types of diseases.

It is known that various HSPs are constitutively expressed in the skin, and their expression, especially that of HSP70, is up-regulated by stressors such as heat treatment (24, 25). UV irradiation of keratinocytes induces the expression of HSPs not only *in vitro* but also *in vivo* (25–29). Furthermore, artificial expression of HSP70 in keratinocytes and melanocytes confers protection against UV not only *in vitro* (24, 29–32) but also *in vivo*; a sensitive phenotype of HSP70-null mice to UV-induced epidermal and dermal damage has been reported (33). Furthermore, protection of the skin against UV by expression of HSP70 has been suggested to occur in human skin (34). Therefore, if HSP70 can suppress melanin production, non-toxic HSP70 inducers should be beneficial as hypopigmenting agents because they can suppress melanin production while simultaneously protecting the skin against UV. It was recently reported that heat treatment of cultured melanoma cells suppresses melanin production; however, the contribution of HSPs to this suppression was not tested (35, 36). In this study we reproduced this suppression in another mouse melanoma cell line (B16) and found that in these cells artificial overexpression of HSP70 also suppresses melanin production. We also found that UVB irradiation-induced production of melanin in the epidermis was suppressed in transgenic mice expressing HSP70. Based on these results, we propose that non-toxic HSP70 inducers will be pharmaceutically and cosmetically beneficial as hypopigmenting agents.

EXPERIMENTAL PROCEDURES

Materials and Animals—Dulbecco's modified Eagle's medium was obtained from Nissui Pharmaceutical Co. [α-^{32}P]GTP (6000 Ci/mmol) was from MP Biomedical. The RNeasy kit and HiPerFect transfection reagent were from Qiagen. PrimeScript® 1st strand cDNA synthesis kit was purchased from TAKARA Bio, and iQ SYBR Green Supermix was from Bio-Rad. Fetal bovine serum), melanin, 3-isobutyl-1-methylxanthine (IBMX), and α-MSH were from Sigma. Dynabeads Protein G, Lipofectamine (TM2000), Alexa Fluor 488 goat anti-mouse immunoglobulin G, and Alexa Fluor 594 goat anti-rabbit immunoglobulin G were purchased from Invitrogen. Antibodies against tyrosinase and actin were obtained from Santa Cruz. Antibodies against HSP70, HSP25, HSP47, HSP60, and HSP90 were from Stressgen. An antibody against MITF was obtained from Thermo Scientific. L-DOPA was from Nacalai, and the Dual Luciferase Assay System and NTP mixture were from Promega. Transgenic mice expressing HSP70 and their wild-type counterparts (8–10 weeks old, male) were gifts from Drs. C. E. Angelidis and G. N. Pagoulatos (University of Ioannina, Greece) and were prepared as described previously (17). Homozygotic male transgenic mice were used in the experiments. The experiments and procedures described here were carried out in accordance with the Guide for the Care and Use of Laboratory Animals as adopted and promulgated by the National Institute of Health and were approved by the Animal Care Committee of Kumamoto University.

Cell Culture—B16 cells were cultured in Dulbecco's modified Eagle's medium supplemented with 10% fetal bovine serum, 100 units/ml penicillin, and 100 μg/ml streptomycin in a humidified atmosphere of 95% air with 5% CO_2 at 37 °C. Transfection of B16 cells with pcDNA3.1 containing the *hsp70* gene (37) was carried out using Lipofectamine (TM2000) according to the manufacturer's protocol. The stable transfectants expressing HSP70 were selected by immunoblotting and real-time RT-PCR analyses. Positive clones were maintained in the presence of 200 μg/ml G418.

Immunoblotting Analysis—Whole cell extracts were prepared as described previously (38). The protein concentration of each sample was determined by the Bradford method (39). Samples were applied to polyacrylamide SDS gels and subjected to electrophoresis after which proteins were immunoblotted with each antibody.

Determination of Melanin Content in Vitro—Melanin content was determined as described previously (40, 41) with some modifications. Cells were homogenized with 1 N NaOH. The melanin content of the cell extracts and the culture medium was determined by measuring the absorbance at 405 nm with a plate reader (Fluostar Galaxy).

Tyrosinase Activity Assay—Tyrosinase activity was assayed as described previously (42) with some modifications. Cells were washed with phosphate-buffered saline and homogenized with 20 mM Tris/HCl (pH 7.5) buffer containing 0.1% Triton X-100. Tyrosinase activity (oxidation of L-DOPA to DOPAchrome) was monitored as follows. Cell extracts (50

balt3/zbc-bc/zbc-bc/zbc02010/zbc1371-10z ZSUBMIT 32 xppws S=1 9/3/10 5:24 4/Color Figure(s) F5,8 ARTNO: M110.103051

μl) were mixed with 100 μl of freshly prepared substrate solution (0.1% L-DOPA in phosphate-buffered saline) and incubated at 37 °C. The production of DOPAchrome was monitored by measuring the absorbance at 475 nm with a plate reader (Fluostar Galaxy) and corrected for auto-oxidation of L-DOPA.

Real-time RT-PCR Analysis—Real-time RT-PCR was performed as previously described (43) with some modifications. Total RNA was extracted from cells using an RNeasy kit according to the manufacturer's protocol. Samples (2.5 μg of RNA) were reverse-transcribed using a first-strand cDNA synthesis kit. Synthesized cDNA was used in real-time RT-PCR (Chromo 4 instrument (Bio-Rad)) experiments using iQ SYBR Green Supermix and analyzed with Opticon Monitor Software. Specificity was confirmed by electrophoretic analysis of the reaction products and by inclusion of template- or reverse transcriptase-free controls. To normalize the amount of total RNA present in each reaction, glyceraldehyde-3-phosphate dehydrogenase (GAPDH) cDNA was used as an internal standard.

AQ: D

Primers were designed using the Primer3 website. The primers used were (forward and reverse primers, respectively): tyrosinase, 5′-cctcctggcagatcatttgt-3′ and 5′-ggttttggctttgtcatggt-3′; *gapdh*, 5′-aactttggcattgtggaagg-3′ and 5′-acacattgggggtaggaaca-3′; *mitf*, 5′-ctagagcgcatggactttcc-3′ and 5′-acaagttcctggctgcagtt-3′.

siRNA Targeting of Genes—We used siRNA with the sequences of 5′-agcaguaccuuucuaccacdTdT-3′ and 5′-gugguagaaagguacugcudTdT-3′ as annealed oligonucleotides for repressing MITF expression. Cells were transfected with siRNA using HiPerFect transfection reagent according to the manufacturer's instructions. Non-silencing siRNA (5′-uucuccgaacgugucacgudTdT-3′ and 5′-acgugacacguucggagaadTdT-3′) was used as a negative control.

Luciferase Reporter Assay—The plasmid, pGL4-tyrosinase-luc (44), was a gift from Dr. M. Funaba (Kyoto University). The luciferase assay was performed as described previously (44, 45). Cells were transfected with 1 μg of each of the *Photinus pyralis* luciferase reporter plasmids (pGL4-tyrosinase-luc) and 0.125 μg of an internal standard plasmid bearing the *Renilla reniformis* luciferase reporter (pRL-SV40). *P. pyralis* luciferase activity in the cell extract was measured using the Dual Luciferase Assay System and then normalized for *Renilla reniformis* luciferase activity.

Co-immunoprecipitation Assay—Immunoprecipitation was carried out as described previously (46) with some modifications. Cells were harvested, lysed, and centrifuged. The antibody against HSP70 or MITF was added to the supernatant, and the samples were incubated for 12 h at 4 °C with rotation. Dynabeads Protein G was added and incubated for 2 h at 4 °C with rotation. Beads were washed four times, and proteins were eluted by boiling in SDS sample buffer.

Immunostaining Microscopy—After fixation with 4% paraformaldehyde, cells were incubated with antibody against HSP70 or MITF for overnight. Samples were further incubated with the respective secondary antibody. We acquired images with a confocal fluorescence microscope (Olympus FV500).

Chromatin Immunoprecipitation Assay—A chromatin immunoprecipitation assay was done as described previously (47) with some modifications. Cells were cross-linked with 1% formaldehyde for 10 min at 25 °C. After the addition of 125 mM (final concentration) glycine, cells were harvested and suspended in the lysis buffer (10 mM HEPES, 1.5 mM $MgCl_2$, 10 mM KCl, 0.5 mM dithiothreitol, 0.1% Nonidet P-40, and protease inhibitors). After 10 min of incubation on ice, cells were centrifuged to pellet the nuclei. Nuclei were then suspended in the nuclei lysis buffer (50 mM Tris/HCl (pH 8.1), 10 mM EDTA, 1% SDS, and protease inhibitors). Samples were sonicated 30 times for 10 s (to achieve an average fragment size of 0.5–1 kb). Immunoprecipitation was performed with magnetic beads that were coated with protein G and antibody against MITF or HSP70. Precipitates were washed, processed for DNA purification, and subjected to real time RT-PCR.

The primers used were (forward and reverse primers, respectively): tyrosinase promoter, 5′-gtctacttatgatctctaaatacaacaggcttg-3′ and 5′-tcatacaaaatctgcaccaataggttaatgagtg-3′; *gapdh*, 5′-acccagaagactgtggatgg-3′ and 5′-cacattgggggtaggaacac-3′.

In Vitro Transcription Assay—*In vitro* transcription assay was done as described (48) with some modifications. Nuclear extracts (5 μg protein) were incubated with DNA fragments containing the tyrosinase promoter and transcribed region (−270/+59) or the glucose-regulated protein (*grp78*) promoter and transcribed region (−304/+253) in the buffer containing 20 mM HEPES/KOH (pH 7.9), 100 mM KCl, 0.5 mM dithiothreitol, 1 mM EDTA, 20% glycerol, 0.4 mM ATP, 0.4 mM CTP, 0.4 mM UTP, 0.016 mM GTP, [α-^{32}P]GTP, and 4 mM $MgCl_2$ for 60 min at 30 °C. Isolated RNAs were resolved by electrophoresis on 15% polyacrylamide gel containing 7 M urea. The gel was dried and autoradiographed.

Assay for Melanin Production in Vivo—Animals were exposed to UVB irradiation with a double bank of UVB lamps (peak emission at 312 nm, VL-215LM lamp, Vilber Lourmat). The energy of the UV was monitored by radiometer sensor (UVX-31, UV Products). Skin reflective colorimetric measurements were assessed with a narrow-band simple reflectance meter (Mexameter MX18, Courage-Khazaka). The measurement was done for four parts of the skin, and the mean was calculated. The measurement area was 5 mm in diameter, and the instrument was calibrated using black and white calibration plates. Skin biopsies were harvested and processed for Fontana-Masson staining, as described (49).

Statistical Analysis—All values are expressed as the mean ± S.D. or S.E. Two-way analysis of variance followed by the Tukey test was used to evaluate differences between more than three groups. Differences were considered to be significant for values of $p < 0.05$.

RESULTS

Inhibition of Melanin Production by Expression of HSP70—As mentioned above, it has been reported that heat treatment of mouse melanoma cells (Mel-Ab) suppresses melanin production (35, 36). In this study we tested whether similar results are observed for a different mouse melanoma cell line (B16). Because UVB irradiation of B16 cells did not stimulate the melanin production (supplemental Fig. S1, *A* and *B*), we used either α-MSH or IBMX (which is a cAMP-elevating agent that acts through inhibition of phosphodiesterase) to mimic UV-stimu-

ZSI

balt3/zbc-bc/zbc-bc/zbc02010/zbc1371-10z ZSUBMIT 32 xppws S=1 9/3/10 5:24 4/Color Figure(s) F5,8 ARTNO: M110.103051

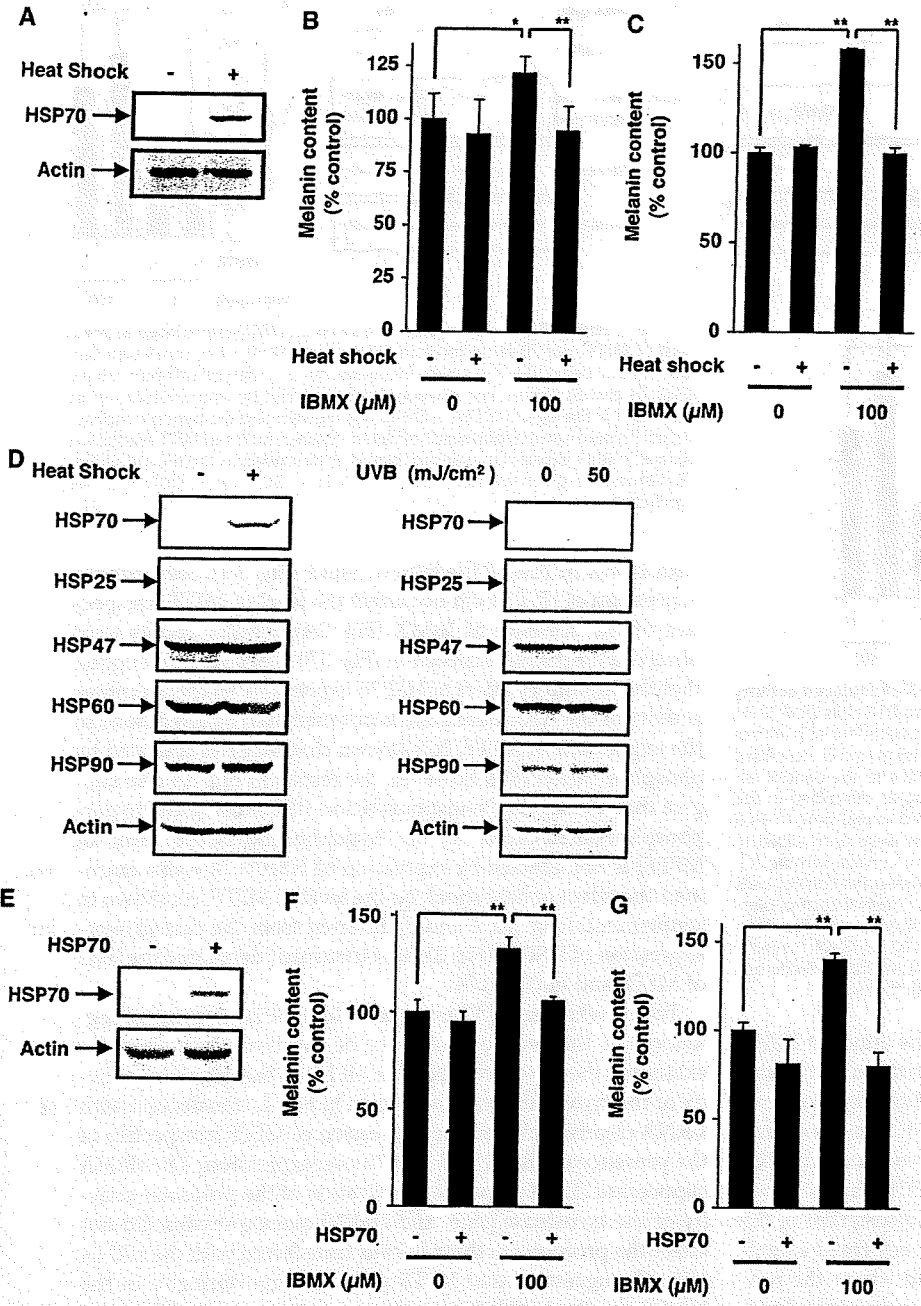

FIGURE 1. **Effect of heat treatment or overexpression of HSP70 on IBMX-stimulated melanin production.** B16 cells were incubated for 1.5 h at 42 °C (*Heat Shock* +) or 37 °C (*Heat Shock* −) then for 6 h at 37 °C and finally for 72 h at 37 °C with or without 100 μM IBMX (*A–C*). B16 cells were incubated for 1.5 h at 42 °C (*Heat Shock* +) or 37 °C (*Heat Shock* −) or irradiated with or without indicated doses of UVB and cultured for 24 h (*D*). HSP70-overexpressing B16 cells (*HSP70* +) and mock transfectant control cells (*HSP70* −) were incubated for 72 h with or without 100 μM IBMX (*E–G*). Whole cell extracts were analyzed by immunoblotting (*A*, *D*, and *E*). The amounts of melanin in the conditioned medium (*B* and *F*) or cell extract (*C* and *G*) were determined as described under "Experimental Procedures" and are expressed relative to the control. Values are given as the mean ± S.D. ($n = 3$). **, $p < 0.01$; *, $p < 0.05$.

lated melanin production *in vivo* and measured the amount of melanin in both the culture medium and cell extract. We confirmed that heat treatment (42 °C, 1.5 h) induced expression of HSP70 (Fig. 1*A*). As shown in Fig. 1, *B* and *C*, treatment of B16 cells with IBMX increased the melanin content in both fractions, and pretreatment of the cells with the heat shock suppressed this increase significantly, suggesting that the heat treatment inhibited IBMX-stimulated production of melanin. We also examined the effect of heat shock on melanin production in cells in which the production had been already activated by IBMX and found that the heat treatment inhibited the melanin production even under these conditions (supplemental Fig. S1, *C* and *D*). Similar results were observed for α-MSH-stimulated production of melanin (supplemental Fig. S1, *E* and *F*). As shown in Fig. 1*D*, this heat treatment also induced the expression of HSP25 weakly but did not induce the expression of other HSPs. We also found that UVB irradiation of B16 cells did not clearly affect the expression of HSPs (Fig. 1*D*).

We established a clone of B16 cells that stably overexpresses HSP70. The extent of expression of HSP70 in this clone is shown (Fig. 1*E*). We confirmed that this overexpression of HSP70 did not affect the cell growth (data not shown). IBMX- and α-MSH-dependent increases in the amount of melanin in the culture medium and cell extract were observed in the control clone but were not so apparent in the clone overexpressing HSP70 (Fig. 1, *F* and *G*, supplemental Fig. S1, *G* and *H*), showing that expression of HSP70 somehow inhibits the synthesis of melanin in B16 cells.

We also examined the effect of heat shock and/or UVB irradiation on melanin production with or without IBMX. As shown in supplemental Fig. S1, *I* and *J*, irradiation with UVB did not affect the melanin production with or without IBMX. UVB did not affect the melanin production even with simultaneous heat treatment (supplemental Fig. S1, *I* and *J*).

Mechanism for Inhibition of Melanin Production by Expression of HSP70—To understand the mechanisms governing inhibition of melanin production by expression of HSP70, we first examined tyrosinase activity. As shown in Fig. 2*A*, treatment of control cells with IBMX increased the tyrosinase activity in the cell extract as described previously (42), and this increase was not observed for cells

balt3/zbc-bc/zbc-bc/zbc02010/zbc1371-10z ZSUBMIT 32 xppws S=1 9/3/10 5:24 4/Color Figure(s) F5,8 ARTNO: M110.103051

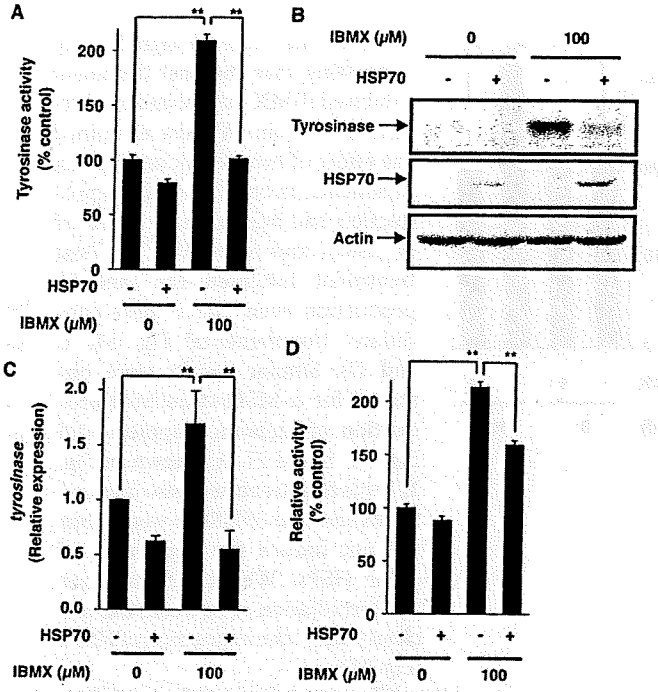

FIGURE 2. **Effect of overexpression of HSP70 on IBMX-stimulated activity and expression of tyrosinase.** HSP70-overexpressing B16 cells (*HSP70* +) and mock transfectant control cells (*HSP70* −) were incubated for 48 h with or without 100 μM IBMX (*A–C*). Tyrosinase activity was determined as described under "Experimental Procedures" and expressed relative to the control (*A*). Whole cell extracts were analyzed by immunoblotting as described in the legend of Fig. 1*B*. Total RNA was extracted and subjected to real-time RT-PCR using a specific primer for the tyrosinase gene. Values were normalized to *gapdh* gene expression and expressed relative to the control sample (*C*). HSP70-expressing B16 cells (*HSP70* +) and mock transfectant control cells (*HSP70* −) were transiently transfected with pRL-SV40 (internal control plasmid carrying the *R. reniformis* luciferase gene) and pGL4-tyrosinase-luc. After 24 h, the cells were incubated for 24 h with or without 100 μM IBMX. *P. pyralis* luciferase activity was measured and normalized for *R. reniformis* luciferase activity (*D*). Values are given as the mean ± S.D. ($n = 3$). **, $p < 0.01$.

overexpressing HSP70. We also examined the effect of IBMX and/or overexpression of HSP70 on the expression of tyrosinase. Treatment of cells with IBMX increased the level of tyrosinase, and this increase was suppressed in HSP70-overexpressing cells (Fig. 2*B*). Similar results were observed at the mRNA level, which was monitored by real-time RT-PCR (Fig. 2*C*), suggesting that expression of HSP70 inhibits transcription of the tyrosinase gene. To confirm this notion, we performed a luciferase reporter assay using a reporter plasmid where the promoter of the tyrosinase gene is inserted upstream of the luciferase gene. As shown in Fig. 2*D*, treatment of cells with IBMX increased luciferase activity in the cell extract, and the activity was significant lower in IBMX-treated HSP70-overexpressing cells than in the control cells, supporting the notion that expression of HSP70 inhibits the expression of tyrosinase at the level of transcription. Results similar to those in Fig. 2 were observed when heat treatment was used for induction of SI expression of HSP70 (supplemental Fig. S2, *A–D*).

As described in the introduction, MITF plays a central role in UV-induced expression of tyrosinase through its specific binding to the promoter of the tyrosinase gene (50). We examined the effect of IBMX and/or expression of HSP70 on the expression of MITF. As described previously (51), treatment of cells

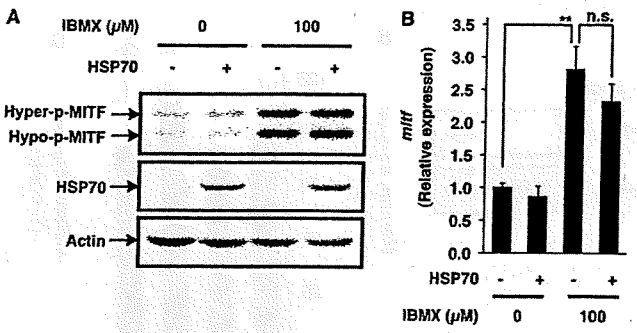

FIGURE 3. **Effect of overexpression of HSP70 on IBMX-stimulated expression of MITF.** HSP70-overexpressing B16 cells (*HSP70* +) or mock transfectant control cells (*HSP70* −) were incubated for 3 h with or without 100 μM IBMX (*A* and *B*). Whole cell extracts were analyzed by immunoblotting as described in the legend of Fig. 1. The bands representing the hyperphosphorylated (*Hyper-p*) and hypophosphorylated (*Hypo-p*) forms of MITF are shown (*A*). *mitf* mRNA expression was monitored as described in the legend of Fig. 2*B*. Values are given as the mean ± S.D. ($n = 3$). **, $p < 0.01$; *n.s.*, not significant.

with IBMX increased the level of MITF (Fig. 3*A*). Surprisingly, F3 expression of HSP70 did not affect the level of MITF irrespective of the presence of IBMX (Fig. 3*A*). Similar results were observed for mRNA expression (Fig. 3*B*). These results suggest that the inhibitory effect of HSP70 expression on the promoter activity of the tyrosinase gene is not mediated by alterations to the expression of MITF. It is known that MITF is activated by phosphorylation (50); however, the results in Fig. 3*A* also suggest that the level of phosphorylation (the ratio of the hyperphosphorylated form to the hypophosphorylated form of MITF) is not affected by expression of HSP70. We also exam- AQ: F ined the effect of heat shock on the level of MITF. As shown in supplemental Fig. S2, *E* and *F*, different from the case of over- ZSI expression of HSP70 (Fig. 3), heat treatment decreased the level of MITF and *mitf* mRNA.

To test whether MITF is required for HSP70-dependent regulation of the promoter activity of the tyrosinase gene, we examined the effect of siRNA for MITF on the promoter activity of the tyrosinase gene. As shown in Fig. 4, transfection with F4 siRNA clearly inhibited the expression of MITF irrespective of the presence of IBMX and HSP70 overexpression. The siRNA suppressed IBMX-dependent activation of the promoter activity of the tyrosinase gene, and HSP70 overexpression did not affect the promoter activity in cells transfected with the siRNA (Fig. 4), suggesting that MITF plays an important role in the inhibitory effect of HSP70 on the promoter activity of the tyrosinase gene.

We also examined the expression of MITF-regulated genes other than the tyrosinase gene, such as tyrosinase-related protein 1 (Tyrp1), dopachrome tautomerase (Dct), and protein phosphatase methylesterase 1 (Pmel). Expression of these genes was enhanced by IBMX and this enhancement was suppressed in HSP70-overexpressing cells (supplemental ZSI Fig. S2, *G–I*).

Involvement of an Interaction between HSP70 and MITF in the Inhibitory Effect of HSP70 on Melanin Production—Based on the results mentioned above and the fact that HSP70 is a molecular chaperone modifying the activity of other proteins by its direct binding, we hypothesized that HSP70 interacts